The Miocene – Pliocene boundary and the Messinian Salinity Crisis in the easternmost Mediterranean: insights from the Hatay Graben (Southern Turkey).

Sarah J. Boulton [a,*], Christopher W. Smart[a], Chiara Consolaro[a, b], Avalon Snider

[a] *School of Geography, Earth, and Environmental Sciences, Plymouth University, Drake Circus, Plymouth, Devon, PL4 8AA, UK*

[b] *CAGE - Centre for Arctic Gas Hydrate, Environment and Climate, Department of Geology, UiT the Arctic University of Norway, Dramsveien 201, N-9037 Tromsø, Norway.*

Abstract

The Hatay Graben is one of three easternmost basins in the Mediterranean that preserve sediments that span the Miocene-Pliocene boundary, including gypsums from the Messinian Salinity Crisis (MSC). Here we integrate existing data and present new sedimentological and micropalaeontological data to investigate the palaeoenvironments of late Miocene to early Pliocene deposits and place this important area into a regional stratigraphic framework. Six sections are described along a ~ W – E transect illustrating the key features of this time period. Late Miocene (Pre-MSC) sediments are characterised by open marine marls with a benthic foraminiferal fauna suggestive of water depths of 100 – 200 m or less. Primary lower gypsum deposits are determined to be absent from the graben as sedimentological and strontium isotopes are characteristic of the resedimented lower gypsums. The intervening Messinian erosion surface is preserved near the basin margins as an unconformity but appears to be a correlative conformity in the basin depocentre. No Upper Gypsums or 'Lago–Mare' facies have been identified but available data do tentatively suggest a return to marine conditions in the basin prior to the Zanclean boundary. Sediments stratigraphically overlying the Messinian gypsums and marls are coarse-grained sandstones from coastal and Gilbert-type delta depositional environments. The Hatay Graben is not only strikingly similar to Messinian basins on nearby Cyprus but also to the overall model for the MSC, demonstrating the remarkable consistency of palaeoenvironments found in marginal basins across the region at this time. This research also raises questions as to the timing of the Mediterranean reflooding and the significance of the widespread mega-breccias of the resedimented gypsum deposits.

Keywords: Messinian Salinity Crisis; Turkey; Eastern Mediterranean; Gypsum; foraminifera; Gilbert-type delta.

1. Introduction

The Messinian Salinity Crisis (MSC) was a dramatic event (~ 5.9 Ma) that affected the whole Mediterranean region when the seaways connecting the Mediterranean Basin to the Atlantic Ocean closed due to uplift in the Bectic Arc/Moroccan Rif region (e.g., Duggan et al., 2003; Sierro et al., 2008). Isolation from the Atlantic Ocean resulted in the deposition of thick evaporite deposits in basin depocentres and significant erosion around the fringes of the Mediterranean. Studies of onshore Messinian strata preserved in basins described as either marginal or peripheral (to the deep, central Mediterranean Basins; Fig. 1) have

* Corresponding author (sarah.boulton@plymouth.ac.uk; fax:01752 233117)

provided much information on the sedimentology, palaeontology and geochemistry of the period, especially when combined with recent high-resolution cyclostratigraphic studies (e.g., Hilgen and Krijgsman, 1999; Sierro et al., 2001; Hilgen et al., 2007; Manzi et al., 2013).

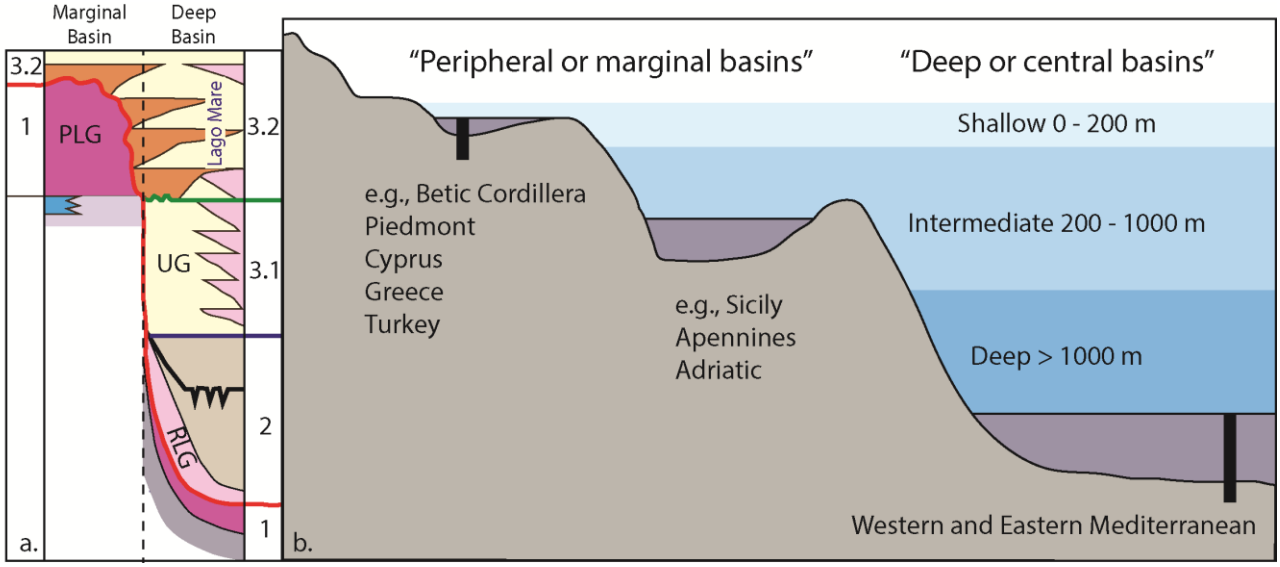

Figure 1. (A) Summary stratigraphic model for the three stages of deposition characteristic of the MSC Crisis in the Mediterranean; PLG - Primary Lower Gypsum, RLG – Resedimented lower Gypsum (modified from CIESM, 2008; Roveri et al., 2014). Note: the numbers (1, 2, 3.1, 3.2) refer to stages of the MSC. (B) Schematic classification of Messinian sub-basins in the Mediterranean (modified from Roveri et al., 2014) showing shallow, intermediate (these basin are also known as peripheral/marginal) and deep water basins.

The MSC resulted in the deposition of characteristic sedimentary units both in marginal (shallow) and deep water environments; however, until recently there were a number of contrasting models that attempted to link marginal and deep basin stratigraphy (Butler et al., 1995; Clauzon et al., 1996; Riding et al., 1998; Krijgsman et al., 1999; Rouchy and Caruso, 2006; Roveri et al., 2008b). A new scenario proposed by the CIESM (the Mediterranean Science Commission) consensus report (2008) develops a correlation scheme that integrates recent sedimentary facies and stratigraphic data from the marginal basins with deep basin seismostratigraphy in order to try to resolve these correlation problems. Furthermore, Roveri et al. (2014a, b) demonstrate that strontium isotope ratios ($^{87}Sr/^{86}Sr$) provide additional stratigraphic constraints as distinct populations of $^{87}Sr/^{86}Sr$ values have been documented during the different phases of the MSC event. This revised Messinian scenario is described within the framework of a 3-stage stratigraphic model constructed mainly with observations from the marginal to intermediate basins exposed onshore in Sicily and in the Northern Apennines (CIESM, 2008; Roveri et al., 2014a, b).

However, despite the extensive 'back-catalogue' of work on the Messinian stage (e.g., Roveri et al., 2014a), many studies from the easternmost extent of the Mediterranean have focussed on Cyprus (e.g., Robertson et al., 1995; Krijgsman et al., 2002; Kouwenhoven et al., 2006; Orszag-Sperber et al., 2006; Manzi et al., 2015) and adjacent ODP data (e.g., Blanc-Valleron et al., 1998; Pierre et al., 1998), with limited data from southern Turkey (Melinte-Dobrinescu et al., 2009; Darbaş and Nazik, 2010; Poisson et al., 2011; Cipollari et al., 2013; Faranda et al., 2013; Radeff et al., 2015). In this paper we focus on late Miocene and early Pliocene sediments of the Hatay Graben (southern Turkey), previously identified by Boulton et al. (2007, 2008) and Tekin et al. (2010). The Hatay Graben is one of the easternmost marginal basins (the other being the Syrian Nahir el-Kabir half-graben) that records evidence from this period, and is the ideal location for investigating the progression of the Messinian salinity crisis and the Zanclean reflooding event in the most distal part of the Eastern Mediterranean basin (Fig. 2). Here we examine key Tortonian, Messinian and Zanclean sections, some of which have been previously documented by Boulton et al. (2007) or Tekin et al. (2010), along with new sedimentological and micropalaeontological data to develop a facies and

palaeoenvironmental model for the Hatay. The aims of the study are to: a) investigate the nature of the Miocene-Pliocene boundary in this marginal basin, b) place these sediments into the revised stratigraphy of the MSC (e.g., CIESM, 2008; Roveri et al., 2014a,b), and c) test the applicability of this model in the easternmost Mediterranean.

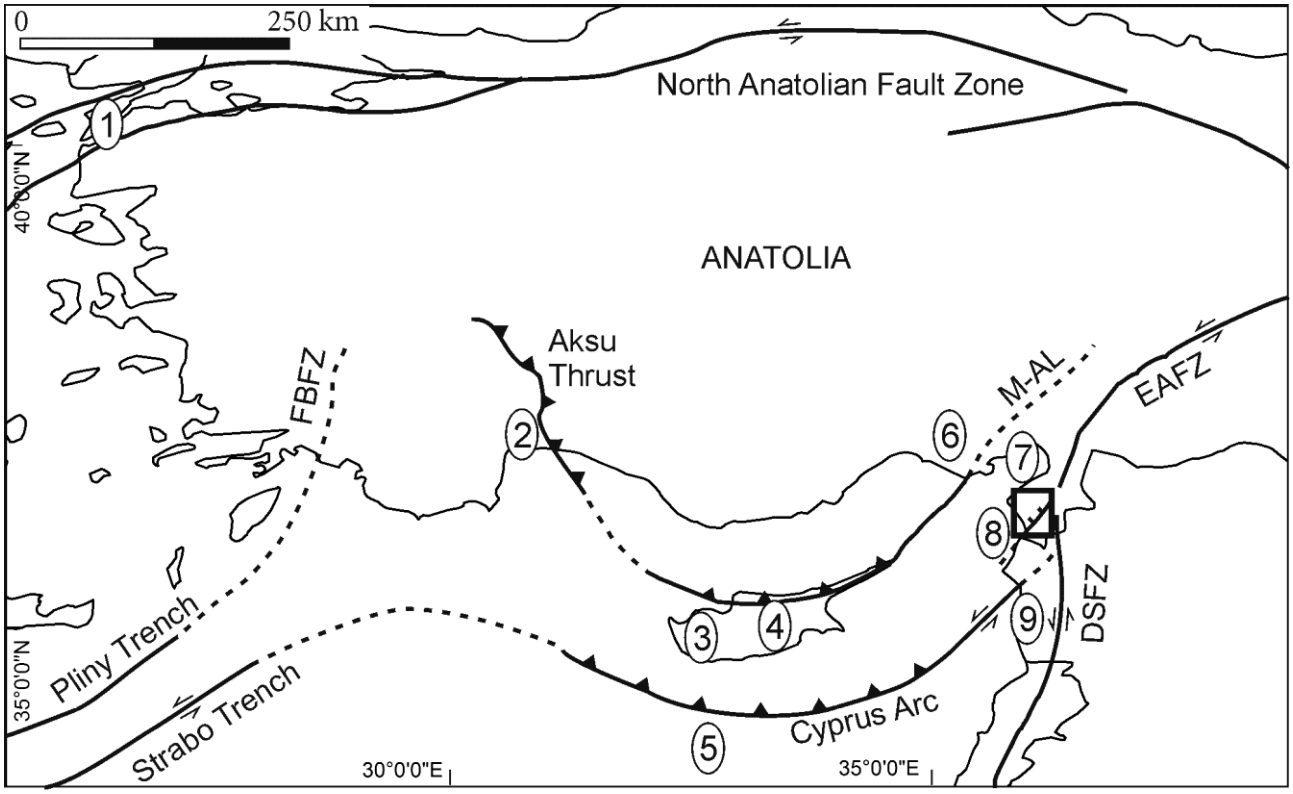

Figure 2. Plate tectonic overview of the Eastern Mediterranean showing the location of key Messinian to Zanclean deposits in the Eastern Mediterranean; EAFZ – East Anatolian Fault Zone; DSZF – Dead Sea Fault Zone; M-AL – Misis-Andirin lineament; FBFZ – Fethiye-Burdur Fault Zone: 1) Dardanelles (Melinte-Dobrinescu et al., 2009); 2) Asparta (Flecker et al., 1998); 3 and 4) Polemi, Pissouri, Maroni and Mesaoria Basins of Cyprus (e.g., Robertson et al., 1995); 5) IODP leg 161 (Iaccarino et al., 1999a, b); 6) Adana Basin, (Darbas and Nazik, 2010; Ilgar et al., 2013); 7) Iskenderun Basin (Tekin et al., 2010); 8) Hatay Graben (this paper; Boulton et al., 2006, 2007; Tekin et al., 2010); 9) Latakia Graben (Hardenberg and Robertson, 2007, 2013).

2. Messinian Stratigraphic Framework

The Global Stratotype Section and Point (GSSP) of the base Messinian is defined as the first occurrence of the planktic foraminifera *Globorotalia miotumida* in the Oued Akrech section (Morocco) at 7.25 Ma (Hilgen et al., 2000). The top of the Messinian is defined by the Zanclean GSSP at Eraclea Minoa (Sicily), coincident with the base of the Trubi marls and the reflooding of the Mediterranean at 5.33 Ma.

The early Messinian (7.25 to 5.97 Ma) is characterised by the change in circulation patterns and water chemistry caused by progressive restriction of the Atlantic-Mediterranean corridors. Early Messinian sediments are usually characterized by cyclical stacking pattern, which include diatomites and sapropels (e.g., Kouwenhoven et al., 2006), and show stepwise reductions in the diversity of planktic foraminifera (Sierro et al., 1999; Blanc-Valleron et al., 2002; Sierro et al., 2003; Kouwenhoven et al., 2006). These changes in diversity have been interpreted as the effect of 400 kyr orbital forcing superimposed on the tectonically controlled closure of the connecting oceanic gateway (Kouwenhoven et al., 2006).

Stage 1 (5.97 – 5.6 Ma) of the MSC is characterised by the widespread onset of evaporite precipitation only in the shallow-water marginal basins (Lugli et al., 2010; Manzi et al., 2013); this unit is termed the *Primary Lower Gypsum* (PLG) (Fig. 1). These deposits typically consist of rhythmically-

deposited gypsum interbedded with shales. Although Vai and Ricchi Lucchi (1977) originally interpreted these as sabkha deposits with subaerial exposure near the top, the recent work of Lugli et al. (2010) concludes that deposition was entirely subaqueous. Below ~ 200 m water depth, in intermediate and deep water basins, lateral facies changes to dolomites and/or barren organic-rich shales have been observed (e.g., Manzi et al., 2007; Lugli et al., 2010; Dela Pierre et al., 2011, 2012). A lack of evaporite deposition in deeper water is possibly due to under-saturation with respect to sulphate in the water column at this time (De Lange and Krijgsman, 2010). The top of the PLG deposits is normally an unconformity termed the 'Messinian Erosional Surface' (MES), the result of regression during the next stage of the MSC. In some marginal basins the MES can cut PLG and older deposits and the correlative conformity of the MES can be traced into deep basins at the base of the RLG unit (Roveri et al., 2008a, b)

Stage 2 (5.6 – 5.55 Ma) represents the acme of the MSC when widespread subaerial erosion took place forming the MES possibly as a result of the high-amplitude base-level fall of the Mediterranean (CIESM, 2008). In shallow marginal basins, subaerial exposure led to erosion and a hiatus of variable amplitude. Eroded material was transported offshore and sediment deposition at this time was dominated by clastic gypsum deposits that form the Resedimented Lower Gypsum unit (RLG; Roveri et al., 2008a, b). A number of factors (i.e., pressure release and fluid migration - Lazar et al., 2012; crustal loading - Govers et al., 2009; tectonic instability – Robertson et al., 1995) have been proposed as the cause of slope instability and gravity failure resulting in mass-wasting deposits and gravity flows of the RLG deposits.

Stage 3 (5.55 – 5.33 Ma) is thought to have been a period of complex water exchange between the Atlantic Ocean and Paratethys (Orszag-Sperber, 2006; Rouchy and Caruso, 2006; Roveri et al., 2008b), which resulted in selenite and cumulate gypsum deposition in shallow marginal basins in the central and eastern Mediterranean (i.e., Sicily and Cyprus). The Upper Gypsum deposits are superficially similar to the PLG deposits, yet facies analysis indicates formation in very shallow water (Manzi et al., 2007, 2009; Lugli et al., 2008; Roveri et al., 2014a). Furthermore, distinctively low Sr isotope values (compared to oceanic values) have been measured from both the gypsum and fossils of these sections, indicating substantial freshwater input (Flecker and Ellam, 2006; Roveri et al., 2014a, b). By contrast, in northern and western marginal basins evaporite-free clastics formed in shallow to deep-water environments with characteristic brackish to fresh water fauna often referred to as the 'Lago Mare' biofacies (Ruggieri, 1967; Bassetti et al., 2004; Orszag-Sperber, 2006; Grossi et al., 2008, Roveri et al., 2008b; Popescu et al., 2015).

The end of the MSC at 5.33 Ma is marked by the return to fully marine conditions and defines the base of the Pliocene epoch (Van Couvering et al., 2000). The boundary is almost universally recognised as a near synchronous flooding surface (Iaccarino et al., 1999a; Gennari et al., 2008) as a result of the catastrophic flood of Atlantic waters into the Mediterranean basin (e.g., Hsu et al., 1973; Blanc, 2002; Meijer and Krijgsman, 2005; Garcia-Castellanos et al., 2009; Periáñez and Abril, 2015). The re-establishment of this Atlantic connection is likely the result of retrogressive erosion of the Gibraltar Strait rather than tectonically driven subsidence (Loget and Van Den Driessche, 2006; Estrada et al., 2011). In many marginal basins, the Zanclean sediments have been recorded as being relatively deep marine facies overlying Messinian evaporites or Lago Mare facies sediments. Gilbert-type fan deltas, possibly of Zanclean-age, are also commonly identified infilling Messinian fluvial canyons cut into underlying deposits (Bache et al., 2012). However, there are outstanding questions on the nature and progression of the 'Lago Mare' event and the Zanclean reflooding, especially regarding the difference between deep and peripheral basins that require further investigation (Popescu et al., 2015).

3. Geological setting and stratigraphy

The Hatay Graben (also known as the Hatay Basin, the Antakya-Samandag Basin, or the Antakya Fault Zone) in southern Turkey is a transtensional half-graben that developed during the late Miocene to Pliocene as a result of the westward extrusion of Anatolia (Boulton et al., 2006; Boulton and Robertson

2008; Boulton and Whittaker, 2009) and the cessation of subduction along the Arabian/Eurasian margin (Robertson et al., 2001). The present day half-graben developed due to the reactivation of basement structures upon a peripheral foreland basin sequence of Miocene age, consisting of lower Miocene fluvial conglomerates (Balyatağı Formation), middle Miocene shelf limestones (Sofular Formation) and upper Miocene (Tortonian) marls and sandy marl (Nurzeytin Formation) (Boulton and Robertson, 2007; Boulton et al., 2007) (Figs. 3, 4). Several Messinian evaporite locations have been identified in the area (Boulton and Robertson, 2007; Boulton et al., 2007; Tekin et al., 2010) forming the Vakıflı Formation (Fig. 3). The Vakıflı Fm. is exposed within the graben margins and also within a perched basin between two normal faults on the southern basin margin (near Sebenoba; Fig. 3). This uplifted location indicates that the main southern graben bounding faults did not yet have significant relief prior to and during the deposition of this unit (Boulton et al., 2006). Therefore, it is likely that during the late Miocene the basin occupied a wider geographic extent than at the present day and may have been connected to the Iskenderun basin to the north (Boulton et al., 2006). Overlying the Vakıflı evaporites is a sequence of Pliocene sandstone and marls (Samandağı Formation) that are exposed only within the margins of the present active graben, suggesting that the boundary faults had developed sufficiently to influence sediment deposition by early Pliocene time (Boulton et al., 2006; Boulton and Robertson, 2008). The base of the Samandağı Formation is variably conformable to unconformable with the underlying Nurzeytin or Vakifli Formations.

The sediments preserved in the Hatay Graben; therefore, allow the investigation into the progression of palaeoenvironments across the Miocene-Pliocene boundary in the easternmost Mediterranean and provide a key test to proposals for a universal stratigraphic model of the basin (CIESM, 2008).

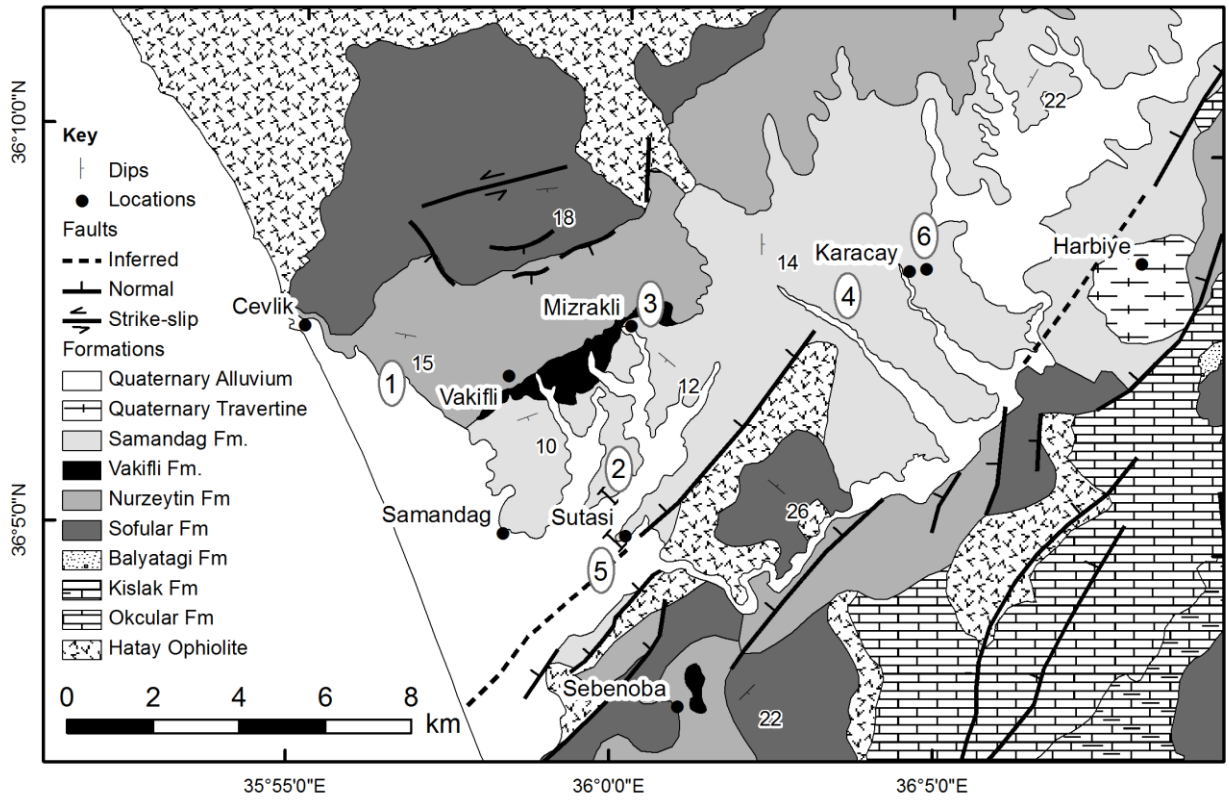

Figure 3. Geological map of the study area showing the location of places and sections described in the text, modified from Boulton et al. (2006) and Tekin et al. (2010). □ Mağaracik Section; □ Ortatepe; □ Mizrakli – Nurzeytin Fm., type section; □ Quarry; □ Sutası Log, □ Road cutting.

4. Methodology

For micropalaeontological analysis, twenty-six marl samples from the Ortatepe Section (location 2, Fig. 3) and four marl samples from location 4 (Fig. 3) were disaggregated using the 'solvent method' of Brasier (1980). The samples were sieved through a 63 µm sieve, dried and benthic foraminifera were picked from the >63 µm size-fraction. In order to determine the minimum number of specimens to be picked per sample, rarefaction curves (number of species versus number of specimens) were calculated for a number of samples. Species-specimen curves become parallel to the species axis at ~150 specimens, so this was considered to be the minimum number of specimens to be picked per sample. In most cases, >200 specimens were picked per sample, although in one case (sample OR7-33) this was not achieved (total 141 specimens) so this sample was excluded from the analysis. Benthic foraminiferal species diversity was recorded in terms of the Fisher's alpha index (Fisher et al., 1943). Alpha index values were read off the base graph in Williams (1964, p. 311) by plotting the number of species against the number of individuals in a sample. The percentage of planktic foraminifera relative to the total foraminiferal assemblage (planktic + benthic) in the >63 µm size-fraction was recorded for each sample. Benthic foraminifera were identified according to Cimerman and Langer (1991) and Milker and Schmiedl (2012).

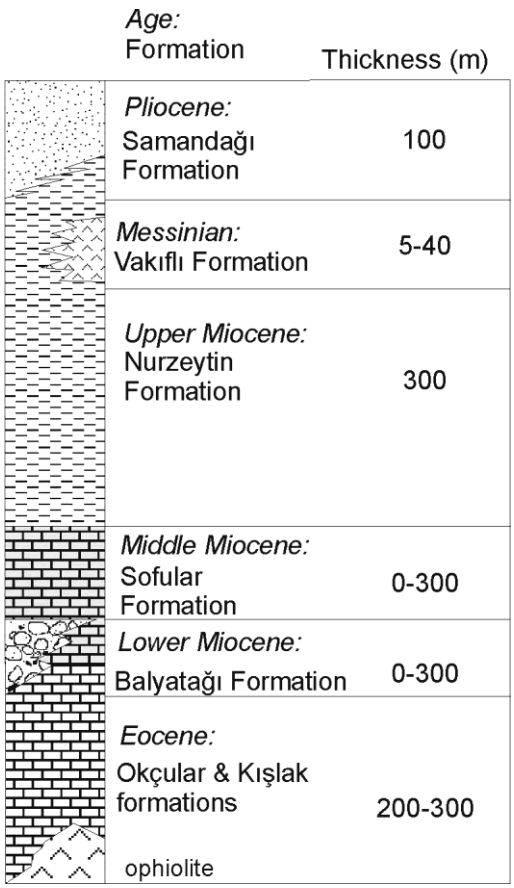

Figure 4. Stratigraphic column for the Cenozoic strata of the Hatay Graben (modified from Boulton et al., 2007).

5. Observations

In this section, six representative sections are described from west to east illustrating the stratigraphy of the late Miocene to Pliocene sediments of the Hatay Graben. Fourteen sedimentary facies (excluding evaporite facies – see Tekin et al., 2010 for a full description of these) have been identified in exposures attributed to Miocene-Pliocene age, detailed sedimentary descriptions and interpretation of each facies is given in Table 1. Facies abbreviations follow convention with G for conglomerates, S for sandstones, M for siltstones and mudstones.

5.1 Mağaracik (Location 1, Fig 3)

Approximately 10 m of cross-bedded, poorly lithified, sandstone is exposed in a strike parallel face in a quarry to the west of Samandağ (Fig. 5; UTM Zone 35 S; 0765400/4000510). These Samandağı Fm., sandstones unconformably overlie the upper surface of the Sofular Formation (middle Miocene limestone), which is eroded and bored at this location dipping down under the sandstone to the east. At the base of the outcrop, the litharenite is medium- to coarse-grained to pebbly (Facies Scr; Table 1) sandstone with bi-directional cross-beds. The outcrop as a whole coarsens upwards with coarse pebbly, cross-bedded sandstone and lenses of conglomerate (Facies Gm; Table 1) present at the top of the section. There is some evidence of bioturbation, as rarely vertical burrows are present, and small fragments of bivalves (e.g., *Ostrea*, *Cardium*) can be observed.

5.1.1 Interpretation

The presence of the small bivalve fragments (*Ostrea*, *Cardium*) indicates a marine origin for these sediments. Coarsening upwards sequences are classic deltaic indicators (Reading and Collinson, 1996), and bi-directional currents are also very common in such environments, typically the result of tidal influences in a shoreface depositional setting. The lower cross-bedded sandstones may belong to the distributary mouth-bar

facies, while the conglomerate lenses could be channel-fill deposits as the delta becomes more fluvially influenced as water depth shallows. Therefore, we interpret this sequence as gravelly-sandy foresets of a Gilbert-type fan delta (Reading and Collinson, 1996).

Facies code	Facies Name	Description	Process	Interpretation
M	Marl	Very fine-grained marl, massive with variable fossil content	Settling from suspension	Background basin deposition
MS	Interbedded mud and sand	Fine-grained sand beds fine upwards into marl/mud. Some of these sand horizons have parallel laminations and scoured bases. There are occasional thin shell lags of fragmented material with abundant scattered bivalves and gastropods.	Low-density turbidity currents – T_d/T_e divisions	Reworked material – storm or turbidite currents
Mp	Mottled mudstone	Mottled mudstones with or without clacliche nodules or root traces	Palaeosols	Subaerial emergence
C	Chalk	Thin bedded limemudstones lacking sedimentary structures	Settling from suspension	Background basin deposition
Sf	Fine-grained sandstone	Grey colour, fossiliferous, miaceous with parallel laminations, vertical burrows and shell/pebble lags.	Upper flow regime laminar flow	Coastal?
Sm	Steeply dipping medium-grained sand	Medium-grained, micaceous, bioclastic calcarenites. Grains are sub- to well-rounded and moderately well-sorted. Beds dip at ~ 20°.	Sediment gravity (Grain) flows	Delta foresets
Smc	Medium-grained contorted sand	Sedimentary characteristics of facies Sm but beds are distrurbed and folded due to syndepositional deformation.	Dewatering or slumping	Downslope instability
Sch	Channelised sands	Medium-grained sand, generally having sharp bases, locally erosional with rip-up clasts, forming small (≤ 5 m wide) channel structures	Bar forms infilling channel scours	Channel infill
Ss	Orange-coloured, greywacke-lithic calcarenite	Medium to coarse-grained sandstone. Bedding planes are sharp and beds fine-upwards occasionally with mud clasts at the base. Sedimentary structures are common, e.g. parallel laminations, cross-lamination, horizontal and vertical burrows, rip-up clasts and lags of shell material and small rounded pebbles but was often disrupted by burrowing (horizontal and vertical; specific types were not identified). Reworked oncolites and rare plant material are also present.	Classic 'Bouma' sequence turbidites.	Turbidites
Sb	Burrowed sandstone	Medium- to coarse-grained, micaceous sandstone. There are numerous of horizontal and vertical burrows, such as *Skolithos*, this intense bioturbation have destroyed sedimentary structures in these sediments, apart from occasional parallel lamination.	Upper flow regime laminar flow?	Foreshore?
Scr	Cross-bedded litharenite	Poorly lithified, medium- to coarse-grained to pebbly litharenite. Grains are sub-angular to rounded and beds generally coarsen upwards	Lower flow regime current flow	Distributary mouth-bar/lower shoreface
S	Coarse-grained lithic-calcarenite	High-angle bi-directional trough cross-bedding is present, along with horizontal parallel lamination and very thin-bedded rippled sandstones.	Unidirectional current flow	Upper shoreface
Gm	Matrix-supported conglomerate	Composed of sub-rounded to rounded, poorly sorted clasts of ophiolitic and carbonate material, which fines upwards into sand. The bases of the beds are erosive forming a channel-like structure (~8m in length), and there is occasional pebble imbrication	Debris Flows	– channel fill deposit
Gc	Fossiliferous Conglomerate	Clast-supported polymict conglomerates composed of well-rounded limestone and ophiolite clasts, some of which have been bored into. The conglomerates are also very shelly with *Ostrea*, bivalves (e.g. *Glycymeris glycyeris*, *Cyclocardia* sp., *Crasostrea* possibly *C.angusta*) and gastropods present	Plunge step? Small channel?	Beach

Table 1. Sedimentological and facies data for the Nurzeytin and Samandağ formations.

Currently the age of these deposits is interpreted as Pliocene, in the absence of other data owing to their stratigraphic position. The basal unconformity is interpreted as the Messinian Erosion Surface that formed during the acme of the MSC as the underlying middle Miocene limestones are highly eroded at this horizon, presumably by a high-amplitude base-level fall during the late Miocene. Therefore, the Samandağı sandstones may have been deposited subsequently possibly during the Zanclean transgression but equally these sediments could date to later in the Plio-Quaternary or to the latest Messinian.

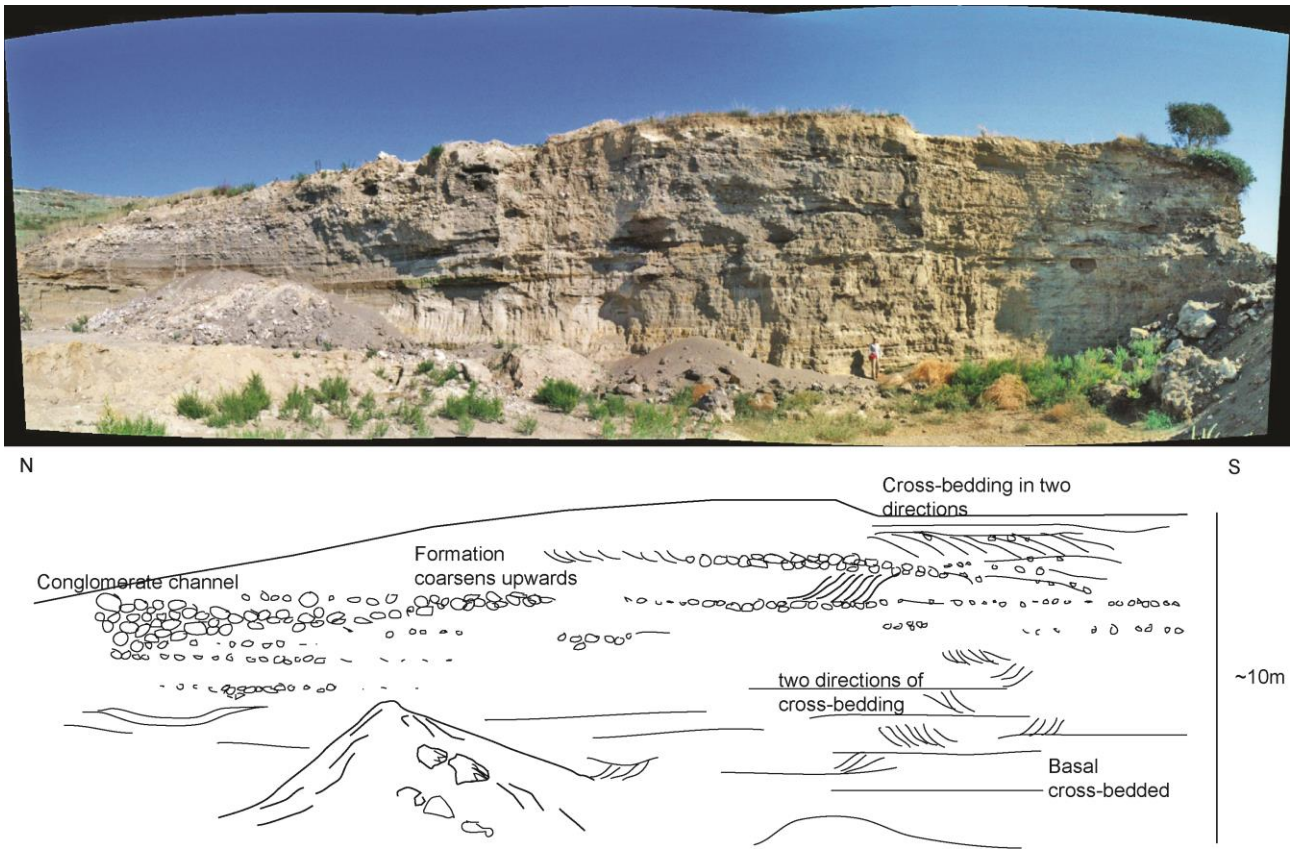

Figure 5. Photograph and sketch of Samandağı Formation sediments of presumed Pliocene age exposed north of Mağaracik (UTM Zone 35 S; 0765400/4000510).

5.2 Ortatepe Section (location 2; Fig. 3)

Incised Quaternary river terraces near the town of Samandağ expose sections of the Nurzeytin and Samandağ Formations. On the eastern side of Ortatepe (UTM Zone 36 S; 769653 E; 3998196 N), excavation to form a field has revealed a exposure ~ 100 m in length and ~ 20 m high, previously described by Boulton et al. (2007). The lower part of the section exposed to the south, is composed of fossiliferous, interbedded, thin (< 20 cm) sand beds and interbedded marl of the Nurzeytin Fm., (Facies M and MS; Table 1) gently dipping to the southeast. The fossil content is variable, with macrofossils such as marine gastropods, including specimens from the Cypraeidae, Ellobiidae and Conidae families, and bivalves including *Ostrea* sp. and *Corbula* sp., present, while microfossils, including ostracods, such as *Cyprideis* spp., *Aurila* spp., and *Loxoconcha* spp., and benthic and planktic foraminifera, including *Globigerinoides* spp., are present near the top of the section (Boulton et al., 2007). Further micropalaeontological analysis (benthic foraminifera) was undertaken on this section as detailed below.

Above the interbedded marl and fine-grained sandstones is an abrupt transisition along a gently dipping planar horizon into medium-grained, massive micaceous sandstone (Facies Sm; Table 1) of the Samandağı Fm., forming moderately dipping (20°) beds that downlap onto the top of the underlying marl (Fig. 6). Above this interval, the lithology is similar but the bedding is disturbed and contorted (Facies Smc; Table 1). Rip-up clasts of parallel laminated mud are present along with horizons of shelly conglomerate containing well-rounded sandstone clasts, bivalves and marine gastropods (e.g., *Neverita josephina*, *Ringicula* sp., *Demoulia* sp., *Calliostoma* sp., *Turris* sp.). Small (~ 5 m) laterally discontinuous beds (Facies Sch; Table 1) and further contorted horizons of facies Smc are present nearby (Facies Smc; Table 1).

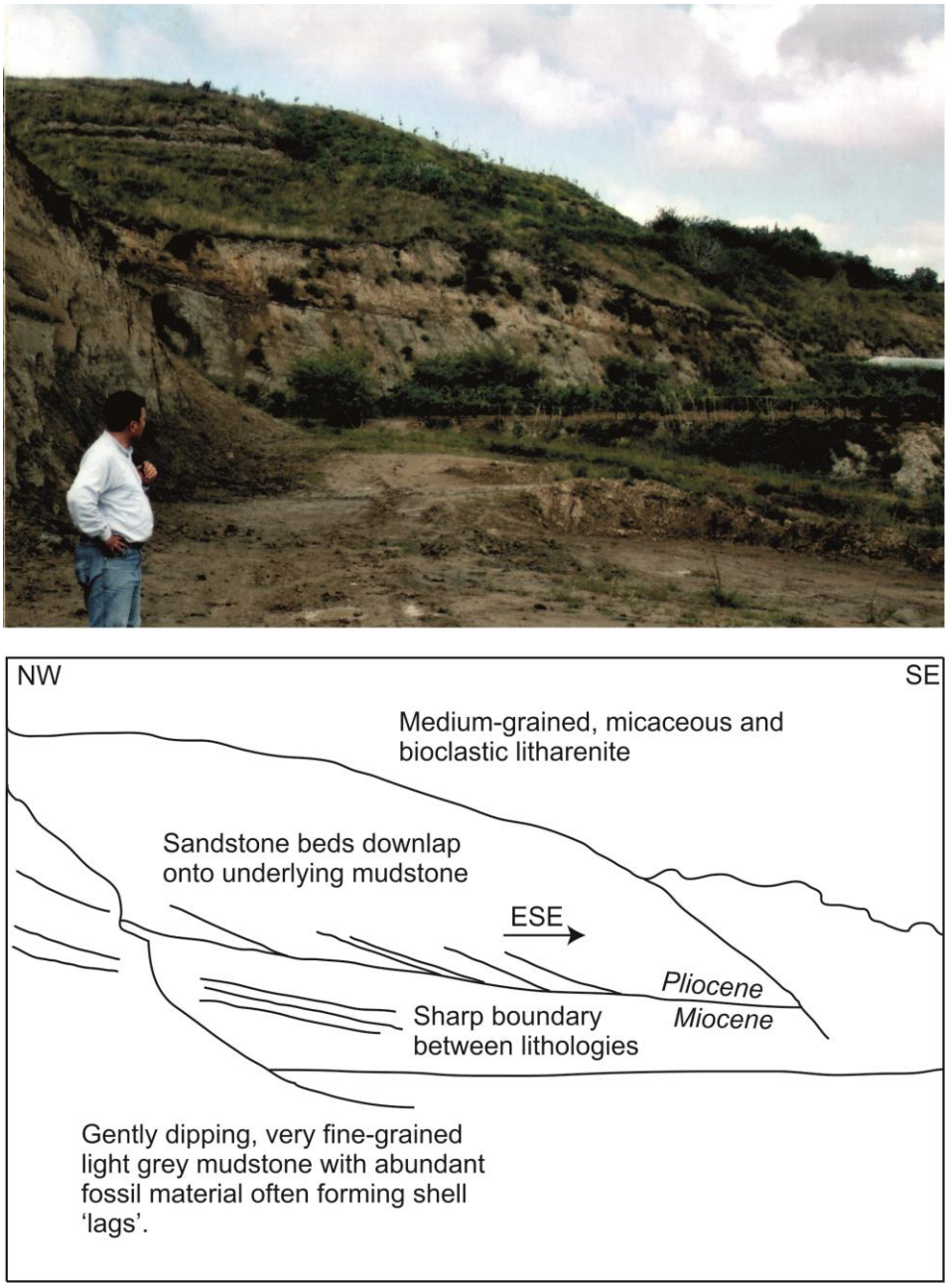

Figure 6. Photograph and field sketch of the downlap surface observed along the terrace at Ortatepe Tepe, where the Pliocene (?) Samandağı Formation overlies the upper Miocene Nurzeytin Fm., (Grid Ref: 0769750/3998399).

5.2.1 Micropalaeontological results

The preservation of benthic foraminifera is generally moderate to good in the majority of samples. Some samples contain broken specimens and some contain specimens with iron staining (OR7-20, 24, 26

and 33). Sample OR7-33, which was excluded from the analysis, contained few individuals, which are poorly preserved and large in size.

The top ten ranked species in all samples overall account for 72.7% of the 107 identified species. The two most abundant species, *Rosalina globularis* and *Asterigerinata mamilla*, occur in every sample and together account for a mean of 33.5% of all species throughout the studied interval. Their relative abundances vary throughout the interval and overall show an increase up through the section (Fig. 7). The percentage of 'high-productivity/low-oxygen species' (sum of % *Bolivina* spp., *Brizalina* spp., *Bulimina* spp., *Melonis affinis* and *Uvigerina peregrina*) (e.g., Lutze and Coulbourn, 1984; Sen Gupta and Machain-Castillo, 1993) shows an overall decrease from mean values of 26% to 14% through the section (Fig. 7). The 'high-productivity/low-oxygen' species group is dominated by *Bolivina* spp. and *Brizalina* spp.; whilst *Bulimina* spp. (0.4% of total), *M. affinis* (0.02%) and *U. peregrina* (0.05%) have very low abundances throughout the studied interval and only occur sporadically. The percentage of miliolids (*Adenosina* spp., *Cornuspira involvens*, *Cycloforina* spp., *Miliolinella* spp., *Pyrgo* spp., *Quinqueloculina* spp., *Spiroloculina* spp.) fluctuates throughout the interval with lower abundances (<2%) occurring in the middle part of the section (OR7-18, 4.25 m to OR7-28, 6.75 m) (Fig. 7). The planktic foraminifera are dominated by small, juvenile specimens in the studied > 63 µm size fraction. Higher percentages of planktic foraminifera occur in the middle part of the section (mean 40%, OR7-16, 3.75 m to OR7-30, 7.25 m) compared with the interval before (mean 25%) and after (mean 25%) (Fig. 7). Diversity fluctuated over the studied interval, although there appears to be a slight temporal trend towards lower values (Fig. 7).

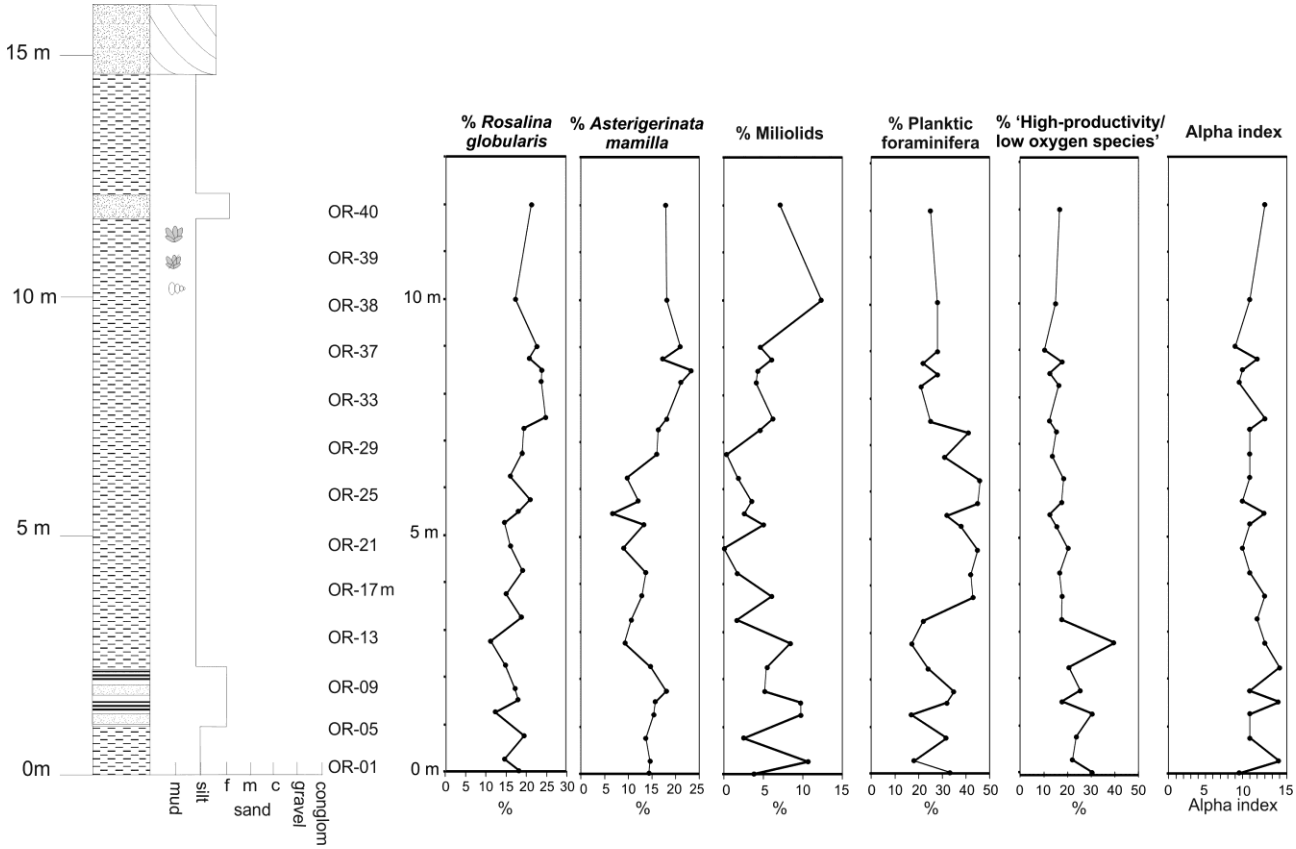

Figure 7. Micropalaeontological results from Ortatepe (location 2; Fig. 3) plus log from the Nurzeytin Formation below the downlap surface seen in figure 6. The key for the log is shown on figure 9.

5.2.2 Interpretation

The benthic foraminiferal assemblages (dominated by *Rosalina*, *Asterigerinata*, *Haynesina*, *Elphidium*, *Ammonia*) indicate that the deposition of the marl succession occurred in an inner shelf environment (0-100 m water depth) (Murray, 1991, 2006). This is supported by the alpha index values (α 9-

15), which fall within the range typical of inner shelf environments (α 3-19) (Murray, 1991). Barbieri and Ori (2000) found a similar benthic foraminiferal fauna dominated by ammoniids, elphidiids and epiphytes from the Neogene of northwest Morocco that they interpreted as indicative of an inner neritic (0-30 m) environment. The percentage of planktic foraminifera, however, could suggest a middle shelf environment (Murray, 1976), and water depths of up to 200 m have been proposed by Boulton et al. (2007). However, the high proportion of juvenile planktic foraminifera supports shallower water depths of middle to inner shelf environments (Murray, 1976). The apparent contradiction in the palaeoenvironmental reconstruction could be a function of the size-fraction used in this study compared with other studies. Many studies calculate the percentage of planktic foraminifera (or P:B ratios) in the >125 μm or >150 μm size-fraction, but our study of the >63 μm size-fraction would potentially overestimate the proportion of planktic foraminiferal specimens, particularly if smaller species and/or juveniles are abundant, compared with larger size-fractions. The increase in the percentage of planktic foraminifera in the middle part of the succession may indicate that the water depth increased at this time, and the concomitant decrease in the abundance of miliolids, which are generally more abundant in shallower water (Murray, 1991, 2006), generally supports this observation.

In the modern Mediterranean Sea, the two most abundant species, *R. globularis* and *A. mamilla*, are known to be epiphytic species that are temporarily attached and make up 10-45% of assemblages on microhabitats with a high sediment content (*Posidonia* rhizomes, algae) (Murray, 2006). It is known that the distribution of epiphytic foraminiferal assemblages is controlled by substrate, light, availability of plant substrates and food (Murray, 2006); therefore the observed changes in the abundance of these species are most likely associated with one or more of these factors. If seagrasses were present, and thus supporting the epiphytic benthic foraminifera, then the maximum water depths allowing photosynthesis would be 20 m (Zieman and Zieman, 1989). The increase in abundance of *R. globularis* and *A. mamilla* up through the section is not likely to be associated with increased food fluxes because the percentage of species indicative of 'high-productivity/low-oxygen' conditions decreases.

When combined with the sedimentary data, the majority of the marl facies of the Nurzeytin Fm. represent background deposition from suspension settling within the basin; the basin floor was possibly colonised by seagrass (*Posidonia* sp.) supporting a benthic community in water depths of < 100 m and maybe < 20 m. The layered nature of the shelly material in the lower marls and thin sandstone beds are suggestive of reworking by high-energy events, possibly storms, turbidity or grain flows, and are characteristic of downslope transport within the basin and may represent a prodelta environment. Prodelta facies associations are typically dominated by low-gradient fine-grained deposits from suspension fall-out and low-density turbidite flows (i.e., Backert et al., 2010), representing the basin environment in front of deltas. The presence of planktic and benthic foraminifera, marine bivalves and gastropods indicates a marine setting for the delta; however, some but not all of the ostracods (Boulton et al., 2007) indicate brackish water conditions (i.e., *Cyprideis* sp). These were likely reworked from the nearshore zone downslope. Evidence for downslope reworking can also be inferred for some foraminifera due to the presence of abraded and/or fragmented tests.

The decimetre-scale beds of the Samandağı Fm., observed to down-lap onto the lower marl and sandstones, represent avalanche foresets of a delta that is prograding into relatively deep water with a high sediment supply from feeder systems (Reading and Collinson, 1996). The disturbed and contorted bedding observed above the foresets is the result of sediment slumping due to downslope instability as a result of either oversteepening of the slope close to the angle of repose by bedload deposition or tectonic activity within the basin. The channelised sands above may represent the lowest-most beds of the subaerial topset of the deltaic system. This facies association is characteristic of a Gilbert-type delta and is remarkably similar to the Gilbert-type deltas described elsewhere in the Mediterranean during the Zanclean (i.e., Melinte-Dobrinescu et al., 2009).

Boulton et al. (2007) identified the Messinian-Zanclean boundary within the marls due to first occurrence of *Globorotalia margaritae* near the top of the section; however, we have found no further age-

diagnostic fauna in this study to corroborate this interpretation. The biota of the marl and sandstone do indicate fully marine conditions, this is supported by the presence upper Miocene ostracods *Cyprideis anatolica* and *C. torosa* and the absence of the post-MSC ostracod *C. agrigentina* (Boulton et al., 2007) used to indicate Lago Mare facies (Faranda et al., 2013). The Ortatepe location is also stratigraphically higher than nearby gypsum outcrops, which all suggests that these marls represent latest Messinian to earliest Pliocene marine conditions in the Hatay Graben. The overlying Gilbert-type delta was therefore deposited subsequently, perhaps during the Zanclean, although we note that the presence of specific facies is not age-diagnostic *per se*.

5.3 Mizrakli (location 3; Fig. 3)

To the east of the villages of Nurzeytin and Mizrakli there is a well-exposed sedimentary succession (as measured from UTM Zone 35 S; 0769443/4003491 to 0230000/4002521) (Boulton et al., 2007). Boulton et al. (2007) report Sr isotope measurements in the range of 0.708878 – 0.708925, confirming a Tortonian age of 8.7 – 9 Ma for the lower to intermediate part of the section. The presence of gypsum deposits at the top of the succession indicates a Messinian age for the end of the section. Although the base of the Nurzeytin Formation is not exposed, the lowermost sediments observed are interbedded grey marl and grey lime mudstone (Facies MS; Table 1). Beds are 30-130 cm thick and fine upwards. The beds are bioturbated and horizontal (to bedding) burrows were observed; fragments of body fossils are also present and include bivalve, gastropod and plant fragments as well as planktic foraminifera. These mudstones are replaced upwards after 10-15 m by a dominantly marl lithology (Facies M; Table 1) with only occasional sandstone interbeds (Facies Ss; Table 1), which occur singly or in packages. Isolated interbeds, often calcarenites <1 m thick, exhibit sharp bases and tops but lack sedimentary structures. Interbeds occurring in packages tend also to be calcarenites, <50 cm thick, with sharp bases, that then fine upwards and grade into a marl bed above. Sedimentary structures such as parallel laminations, cross-laminations, ripple marks, flute casts and rip-up clasts are present. Additionally slumped horizons are present (Facies Smc; Table 1). The top of the logged sequence is capped by ~ 10 m of gypsum following a poor exposed interval of marl. The lower part of the gypsum sequence is formed of 5 m of *in situ* bedded selenite, overlain by a gypsrudite formed of large angular blocks (>2 m) laminated alabastrine and selenite gypsum supported in a matrix of gypsiferous sandy marl.

5.3.1 Interpretation

The Tortonian marls represent settling from suspension within a basinal setting. The water depth is difficult to calculate but probably initially exceeded 100 m in depth (Boulton et al., 2006). The interbeds of calcarenite observed likely represent low density turbidite deposits based upon the range of sedimentary structures present and the overall fining-upward nature of the beds. The presence of turbidity currents along with slumped beds is indicative of down-slope transport of sediments that would have reworked material from the near-shore environment into deeper water. Unfortunately, the lack of palaeocurrent indicators does not allow discrimination between transport offshore into the Levant Basin or into the local basinal depocentre.

The marls pass apparently conformably upwards to Messinian gypsum deposits, although the boundary is not exposed. The gypsum rudite beds, composed of broken selenite crystals, are interpreted as the result of mass flows in a slope setting. Tekin et al. (2010) suggested that tectonic activity at the basin margin could have initiated these flows but did not rule out climatic or water level fluctuations leading to slope instability. The upper chaotic unit is interpreted by Tekin et al. (2010) as the result of active tectonics, by comparison to similar facies reported by Robertson et al. (1995) from southern Cyprus and by Manzi et al. (2011) in Sicily.

5.4 Main Road Quarry Section (location 4; Fig. 3)

On the main Antakya-Samandağ road, a small quarry (UTM Zone 35 S; 0237433/4004350) reveals the contact between the Nurzeytin and Samandağ Formations (Fig. 8). The base of the quarry is composed of blue-grey marls (Facies M; Table 1) and fining upwards beds of very fine-grained sandstone 20 – 50 cm thick (Faces MS; Table 1). Fragmented woody material is common within these sandstone beds but sedimentary structures are lacking. The boundary between the Nurzeytin Fm., marls and the overlying orange-weathering sandstones of the Samandağı Formation is erosive with a slight angular discordance. The coarse-grained sandstones are up to 30 cm thick, dip towards the southwest, and are laterally discontinuous.

Micropalaeontological analyses of the benthic foraminifera on four samples (MBP 1-4) from the underlying Nurzeytin Formation show generally poor preservation with high number of undetermined and reworked (as determined due to abrasion and/or fragmentation) specimens (about 22%). The assemblages are dominated by *Bolivina* spp. and *Brizalina* spp. (together about 30%), where *B. spathulata* (13%) and *B. dilatata* (5%) are the most abundant species. Other relatively common species are *Bulimina* spp. (5.2%, dominated by *B. aculeata* and *B. elongata*), together with *Cibicides lobatulus* (5%), *Cibicidoides* spp. (4.7%), *Cassidulina obtusa* (3.7%), *Eponides* spp. (3.2%), *Rosalina* spp. (3.1%), *Gyroidinoides* spp. (2.2%), *Valvulineria* spp. (2.2%), *Anomalinoides* spp. (2.1%), and *Globocassidulina subglobosa* (2.0%). Others species with abundances of between 1 and 2% are *Fursenkoina* spp., *Ammonia* spp., *Epistominella vitrea*, and *Melonis affinis*, whereas miliolids, *Elphidium* spp., *A. mamilla* and *Uvigerina* spp. are less than 1%. Planktic foraminifera (including *Turborotalita multiloba and Neogloboquadrina acostaensis*) are quite abundant, comprising about 50% of the total foraminifera.

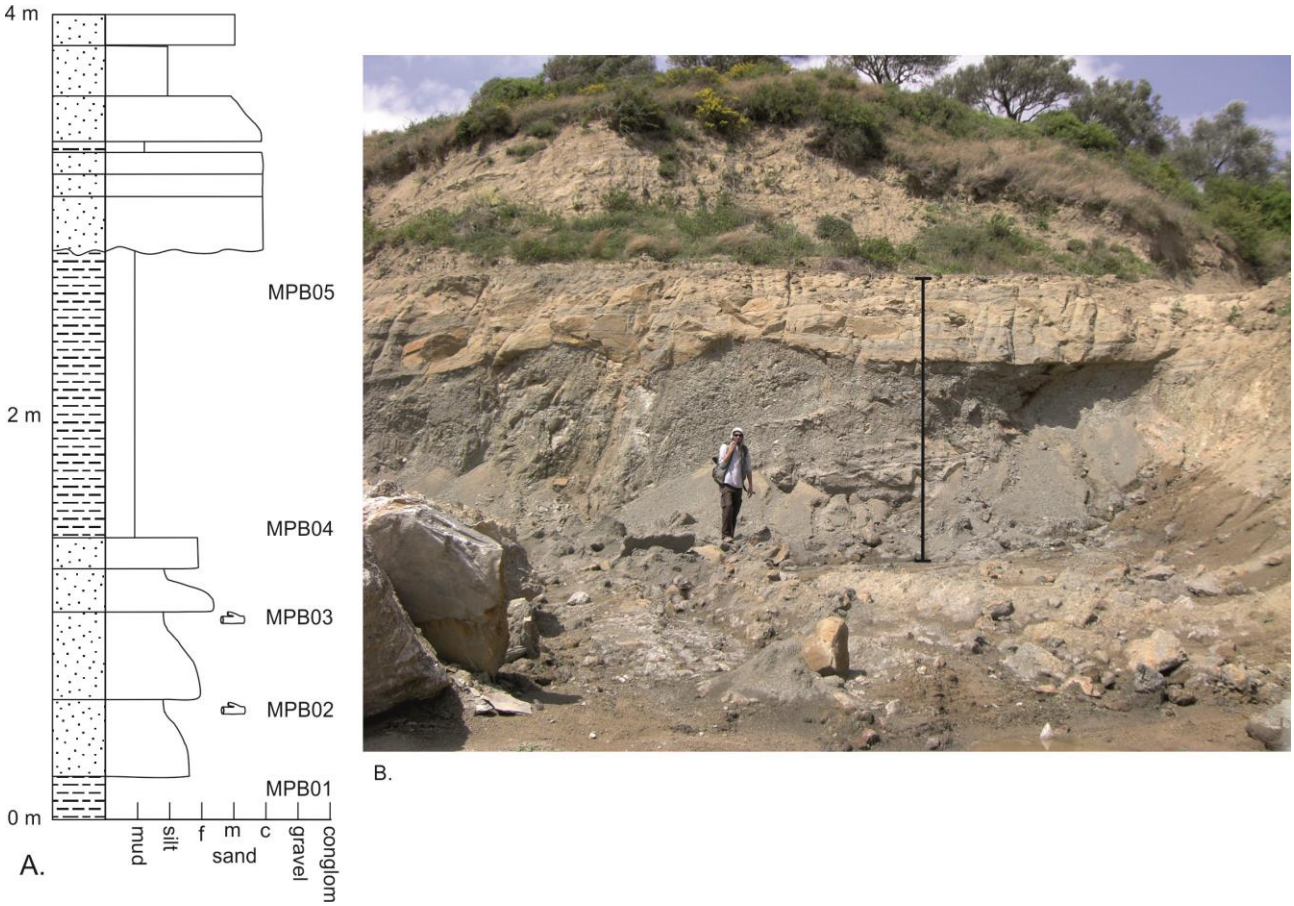

Figure 8. (A) Sedimentary log of Miocene-Pliocene boundary section observed on the Antakya-Samandağ road (location 4; Fig. 3) showing location of samples taken for microfossil analysis – key is shown on figure 9. (B) Photograph of the section, with location of the logged section indicated with the arrow, Note: the slight angular discordance between the lower Nurzeytin Formation and the overlying Samandağı Formation.

5.4.1 Interpretation

The benthic foraminiferal assemblages (dominated by *Bolivina* and *Brizalina*, together with *Bulimina*, *Cibicides*, *Cibicidoides* and *Cassidulina*) indicate that the deposition of the lower part of the succession occurred in an outer shelf-upper slope environment (100-200 m water depth) (Murray, 1991, 2006). This is supported by a high abundance of planktic foraminifera (about 50%), which is typical for this environment. The high percentage of 'high-productivity/low-oxygen species' (especially *Bolivina* spp., *Brizalina* spp., and *Bulimina* spp.), clearly indicate a low oxygen environment with high flux of organic matter (e.g., Lutze and Coulbourn, 1984; Sen Gupta and Machain-Castillo, 1993). The planktic foraminifera *Turborotalita multiloba* is probably an ecophenotypic of *Turborotalita quinqueloba*, and according to Krijgsman et al. (1999), Sierro et al. (2001) and Lourens et al. (2004) its first influx occurs at 6.42 Ma, predating the *Neogloboquadrina acostaensis* sinistral to dextral coiling change at 6.35 Ma. The presence of *N. acostaensis* dextral in the samples confirms that the studied interval belong to the MMi 13c *T. multiloba* Interval Zone spanning from 6.35 Ma to 5.96 Ma (Lourens et al., 2004), which is the last Mediterranean Biozone in the Messinian before the non-distinctive zone corresponding to the MSC.

The overlying sandstone beds of the, presumably Zanclean, Samandağ Formation cut stratigraphically downwards to the southwest (seawards) and are lacking in fossil material. The similarity of these sandstones to the upper sands present in the other described localities implies that these could be the topset beds of a fan-delta system.

5.5 Sutası Section (location 5; Fig. 3)

A well-exposed section of the Samandağ Formation dating to the latest Miocene to earliest Pliocene (Boulton et al., 2007) is exposed near Sutası (Fig. 3, location 2) along a road cutting ~ 650 m long and ~ 10 m high. The base of the section is dominated by fossiliferous, orange-coloured, lithic calcarenite (Facies Ss; Table 1), with bedding thickness 0.25-3.00 m thick (Fig. 9a). Shell fragments are common and are mostly composed of bivalve and gastropod fragments with occasional articulated bivalves forming shell and pebble lags. Preliminary analyses of the benthic foraminifera from the Sutası section show that the assemblages are dominated by *Ammonia* spp., together with *Nonionellina* spp., *Elphidium* spp., *Cibicides refulgens*, *Asterigerinata mamilla*, *Rosalina globularis*, and others. Planktic foraminifera are also present, comprising <25% of the total foraminifera. Ostracods are also represented by *Cyprideis torosa, C. anatolica, Aurila convexa, A. speyeri, Ruggieria tetraptera* and other long lasting species (Boulton et al., 2007). Fragmentary plant material is also present. Interbedded with these sands are thin mud and limestone layers < 25 cm thick.

There is a change in the character of the sediments at ~ 30 m up the section (Fig. 9a); the lithic calcarenite becomes coarser-grained with common trough and planar cross-bedding (Facies Scr; Table 1), yet the thickness of the bedding decreases with many beds <10 cm thick. The overlying beds exhibit planar cross-bedding, parallel-laminations and ripple cross-lamination. These are interbedded with two lenticular polymict clast-supported conglomerates up to 75 cm thick (Facies Gc; Table 1) with coarse sandstone and a 1 m thick mottled pink mudstone above (Table 1). Bioturbation is generally absent in this interval and, as a result, sedimentary structures are well preserved. Macrofossil and microfossil material is very rare and fragmented when present.

Above this interval of diverse structures, the uppermost part of the sequence is composed of > 15 m of medium-grained sandstone with little or no fossiliferous material and mostly lacking in sedimentary structures, although low-angle cross-bedding can be observed in some horizons (Facies Sb; Table 1). This massive sandstone characterises the majority of the Pliocene succession in many outcrops and is generally variably cemented with nodules (similar to doggers) present throughout.

5.5.1 Interpretation

The lower part of the section is composed of medium-grained sandstones with sharp, often erosional, bases that fine upwards, with parallel-laminations and planar cross-lamination in some horizons. Pebble and fossils lags are also commonly present formed as a result of low-relief scours and currents. The bioturbation suggests that between phases of rapid deposition sedimentation was relatively slow allowing colonisation of the substrate. This facies association is typical of coarse-grained lower shoreface environments (Reading and Collinson, 1996; Clifton, 2006).

The lower shoreface passes vertically upwards into the upper shoreface facies association with trough cross-bedded sandstones, the result of oscillatory motion related to the primary onshore waves and secondary back-flow or the result of tidal influences (Dashtgard et al., 2012). The observed increase in grain-size is also common from the lower to the upper shore face (Reading and Collinson, 1996).

The progradational nature of this sequence suggests that the stratigraphically higher sediments would be representative of the foreshore and beach. This interpretation is supported by the presence of horizontal laminations, developed by wave swash and low-angle tabular cross-bedding. The conglomerate lenses could represent the plunge step marking the transition from the top of the shoreface to the base of the foreshore (i.e., Sanders, 2000) but the association of the conglomerate with the pink mudstone suggests that these are more likely to represent small channel fills with an associated palaeosol (as indicated by the mottled colour) indicating a period of subaerial emergence with fluvial erosion and sedimentation. The lack of sedimentary structures resulting from the intense bioturbation in the overlying lithic calcarenite makes the environment of deposition difficult to infer; however, given the overall shallowing upwards sequence these may represent deltaic or fluvial facies. Therefore, the section as a whole would represent a prograding shoreline.

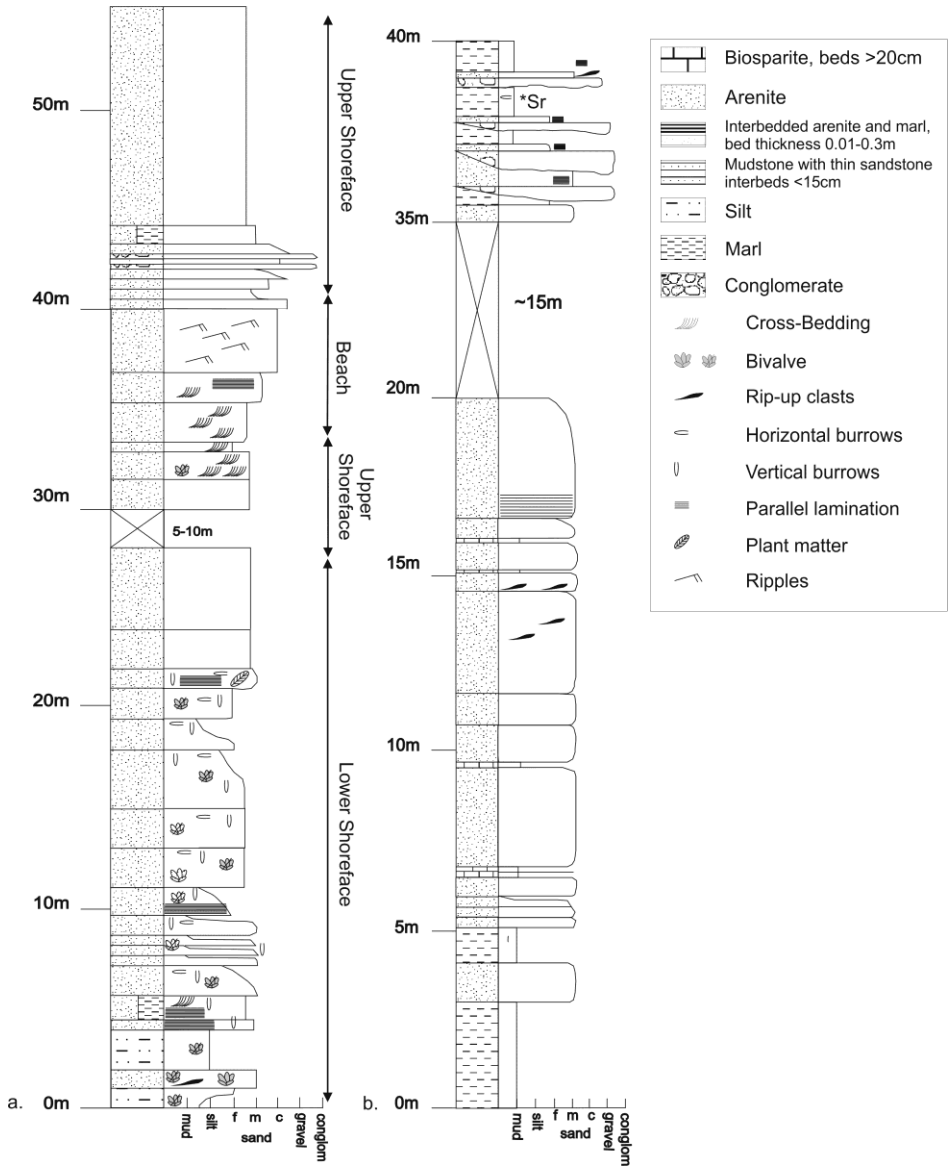

Figure 9.Two sedimentary logs of the Samandağı Formation (A) Log of the Sutası Section (modified from Boulton et al., 2007). (B) Log of location 6 (Fig. 3), showing the stratigraphic position of the Sr measurement reported by Boulton et al. (2007). Key shown is for all logs.

5.6 Location 6 (Fig. 3)

Location 6 is a mixed clastic and carbonate sequence at the base of the Samandağ Formation, the top of this section has been dated using strontium isotopic ratios from benthic foraminifera to 5.35 ± 0.1 Ma (Sr measurement = 0.709023; Age range = 5.2 – 5.41 Ma; Boulton et al., 2007), placing this section within error of the Miocene-Pliocene boundary. However, caution must be applied with strontium ages from the Messinian as a wide range of values occur due to a lack of connection with the global ocean, but by the early Zanclean the return to fully marine conditions results in more robust dates (Flecker and Ellam, 2006). Here, marine conditions are indicated by the presence of a mixed benthic foraminiferal assemblage used to derive the strontium measurement but the marginal setting could still influence the Sr values and thus the derived age.

The basal part of the section is composed of interbedded calcarenite, chalk and marl (Fig. 9b) forming a conformable transistional boundary with the underlying Nurzeytin Formation (Facies M,C, Ss; Table 1). The sandstone is medium-grained and unlithified. Bedding thickness is 0.3-3.0 m. Sedimentary structures are rare, but parallel laminations and rip-up clasts are present, especially near the base of sandsone

beds. The chalk horizons are very thin (5-15 cm). The marl is burrowed and forms the lowermost bed of the section.

The upper part of the section consists of interbedded marl, sandstone and conglomerate. The conglomerates are irregular with erosive bases and are laterally discontinous. The conglomerates are clast supported and clasts are sub-angular to sub-rounded. Above the conglomerates there are fine-grained micaceous lithic greywacke beds with parallel laminations. The bases of these beds are sharp and occasionally erosional; the beds often fine upwards and are generally laterally discontinuous on an outcrop scale. These are capped by marl beds, containing planktic foraminifera (Boulton et al., 2007), completing a upwards fining unit.

5.6.1 Interpretation

These sandstone beds are interpreted as redeposited material. In the lower part of the section, these may be grain-flow and turbidite deposits (Stow et al., 1996), whereas in the upper part of the section the sands may represent channel-fill deposits with basal conglomerate lags. This suggests an increase in energy upwards possibly due to shallowing of the water column. This is in agreement with a decrease in marl up the section that would represent background basin sedimentation (Stow et al., 1996). The Sr isotope value (Boulton et al., 2007) derived from marls near the top of the exposure indicate marine deposition in the basin after the end of the MSC. The mean age places the section just prior to the Messinian-Zanclean boundary, but the error in the measurement does not rule out deposition in the earliest Pliocene.

5.7 Messinian Gypsums

In addition, to the selenite and gypsum breccia observed capping the top of the Mizrakli sequence (section 5.3), gypsum outcrops at a number of other localities in the Hatay Graben (Fig. 3) mainly along strike between the villages of Mizrakli and Vakıflı, and can reach 30 – 40 m in thickness. Typically the sequence consists of a lower alabastrine gypsum with laminations and thin interbedded marl horizons. Often the alabastrine gypsum can be observed to be interbedded with *in situ* selenite. These alabastrine gypsums are normally overlain by gypsum breccias and blocks of gypsum in a gypsiferous marl matrix (Fig. 10). On the southern margin of the graben near Sebenoba (Fig. 3) only the gypsum beccias were observed, consisting of clast-supported blades of selenite with minor gypsiferous marl matrix. Tekin et al. (2010) undertook detailed facies analyses of the evaporites of the Hatay Graben. Their analysis is consistent with our observations and shows that the gypsum deposits in the Hatay Graben can be divided into two sequences; a lower interbedded unit and an upper chaotic unit. The lower sequence is formed of interbedded laminated gypsum, selenite and bedded clastic gypsum facies (Tekin et al. 2010). The laminated gypsum facies is composed of eroded and resedimented gypsum crystals with slumps, normal and reverse grading present. Tekin et al. (2010) interpret these laminate deposits as having been deposited by turbidity or gravity flows in the central part of a density stratified basin (Warren., 2006). The bedded gypsum facies are composed of poorly sorted, massive gypsarenites and gypsrudies with broken selenite crystals up to 4 cm in length, and are also interpreted as having been deposited by mass flows (Tekin et al., 2010). By contrast, the selenite facies is interpreted to have grown *in situ* water depths of > 10 m (Tekin et al., 2010). The upper chaotic unit, as observed at Mizrakli (Fig. 10), is composed of large blocks of selenitic gypsum in a gypsiferous marl matrix with evidence of slumping indicative of down slope transport, which Tekin et al. (2010) attribute to intense tectonism during deposition.

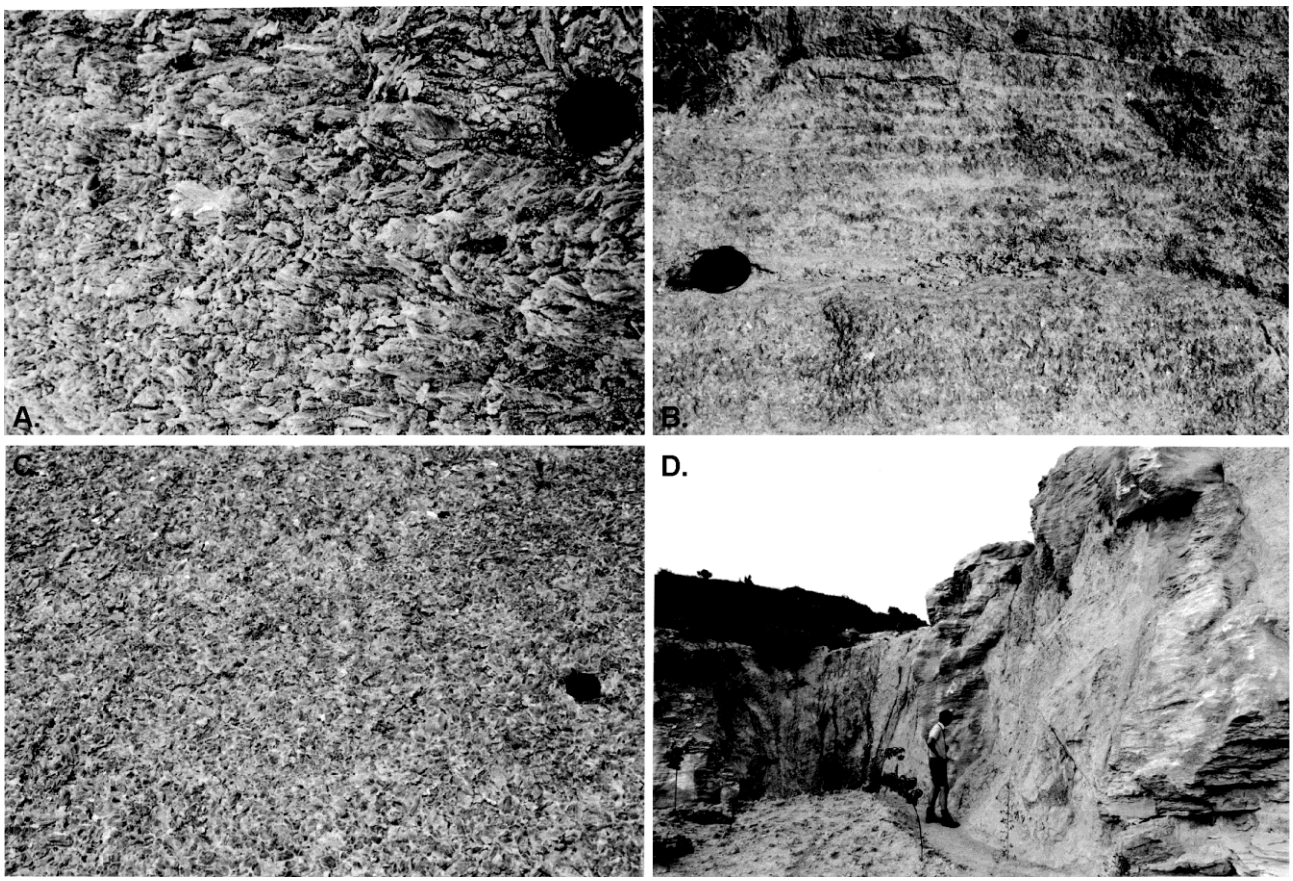

Figure 10. Photographs illustrating gypsum facies of the Hatay Graben. A) Coarse-grained in situ selenite crystals up to 4 cm long and B) laminated and interbedded in situ selenite and alabastrine from near Mizrakli, C) Fine-grained reworked selenite crystals from Sebenoba. Note the lens cap (5 cm diameter) for scale on each photograph. D) large alabastrine blocks in a gypsiferous marl matrix forming the 'mega-breccia' as observed near Vaklıflı.

6. Discussion

6.1 Timing of deposition of the Vakıflı Formation

A key issue when interpreting the sedimentary succession regards timing of gypsum deposition. Do these sediments represent facies of the Primary Lower Gypsum (PLG), the Resedimented Lower Gypsum (RLG) or the Upper Gypsum (UG)? Lugli et al. (2010; p. 84) state that the PLG and RLG deposits of Sicily '*are never associated laterally or vertically*', and therefore the gypsums must represent one or other situation and not both in this model, if it is correct.

Tekin et al. (2010) report two $^{87}Sr/^{86}Sr$ values for the Hatay Graben gypsums: $0.708954 \pm 4x10^{-6}$ and $0.708946 \pm 4x10^{-6}$; although the vertical position within the sections was not stated, it appears that both samples were from the lower interbedded gypsum deposits based upon facies descriptions. These values are entirely consistent with values for the PLG and RLG derived from elsewhere in the Mediterranean that span the range 0.708893 – 0.709024 (Lugli et al., 2010; Roveri et al., 2014b). These data are distinct from values derived from the later UG deposits (typically $^{87}Sr/^{86}Sr$ = 0.708750- 0.708800; Roveri et al., 2014b). These data strongly suggest that the lower interbedded unit in the Hatay basin correlates to the PLG or RLG and therefore the overlying gypsum mega-blocks will also belong to the same unit. The sedimentary characteristics of UG deposits are also distinct from those of the Vakıflı Fm, and therefore can be ruled out.

Tekin et al. (2010) describe two main gypsiferous facies associations in the Hatay Graben. The lower facies association is interpreted as part of a 'sulphate platform'; the upper facies association as an 'evaporitic slope-platform'. However, the sedimentology of both of these facies associations indicates downslope transport of material, initially by grain flows and turbidity currents in the lower bedded units and then by

debris flows in the upper unit forming the 'mega-blocks'. This evidence points towards the reworking of the gypsum characteristic of the RLG facies. These facies are strikingly similar to those described on Cyprus as the lower and intermediate gypsum unit, recently reinterpreted by Manzi et al. (2015) as belonging to the RLG deposits.

Typically, this observation would place the Hatay Graben into the 'marginal' basin class of deeper water basins where RLG facies have been observed (i.e., Sicily: Roveri et al., 2008a; Manzi et al., 2011). However, these observations are at odds with the presence of an unconformity (i.e., location 1) and the microfossil data indicating water depths of < 200 m prior to and in the early Messinian. These features are characteristic of shallow water 'peripheral' basins where PLG typically would have accumulated.

This contradiction may be resolved by considering the tectonic controls on basin formation. Boulton et al. (2006) demonstrated that high-angle oblique normal faulting initiated during the latest Miocene to Pliocene. As a result, footwall uplift and hangingwall subsidence would have (relatively) rapidly produced areas of varying water depth and new depocentres during the Messinian. Therefore, it is possible that in a relatively short time the basin could have deepened sufficiently, combined with seismicity, to rework shallow gypsum facies into basin depocentre to form RLG facies. While on the flanks of the graben PLG facies would have accumulated. In the Hatay basin, shallow water gypsiferous sediments are not preserved but they are farther to the north (Tekin et al., 2010). Therefore, on balance, the Vakıflı evaporites can be considered as RLG deposits but further research into field relationships and strontium isotopes is required to confirm this hypothesis.

6.2 Comparison to other eastern Mediterranean marginal basins

Although the Hatay Graben is located in the easternmost Mediterranean, a number of other basins nearby expose Messinian-aged strata that can increase the understanding of the regional palaeoenvironments of the MSC in the easternmost Mediterranean and aid in the interpretation of the Hatay Graben facies.

Almost due south of the Hatay Graben lies the Nahr El-Kabir half graben in present-day Syria where outcrops of Messinian evaporites up to 100 m thick have been documented (Hardenberg and Robertson, 2007). Underlying Tortonian sediments are generally absent or very thin, suggesting limited accommodation space in this region prior to the onset of the MSC; this is somewhat different to the shallowing but significant water depth in the Hatay. Hardenberg and Robertson (2007) describe the Messinian gypsums as having a tripartite subdivision with a lower unit comprising mainly alabastrine-type gypsum with marl laminations, a middle selenitic division, and an upper matrix-supported conglomerate. These deposits are interpreted as deposition in local depocentres with the uppermost unit the result of tectonic instability (Hardenberg and Robertson, 2007). Indeed, to generate the required accommodation space to accumulate these thick evaporite deposits, tectonic subsidence needs to be invoked given regional base-level fall. Although, strontium data are lacking for this area, the stratigraphy is similar to that described for the Hatay Graben, indicating that the gypsums in the Nahir El-Kabi half-graben could belong to the RLG.

Similar successions have been described for the Messinian evaporites in a number of sub-basins on Cyprus – the Polemi and Pissori sub-basins in the west and the Maroni sub-basin in the south (e.g., Eaton, 1987; Follows, 1992; Payne and Robertson, 1995; Robertson et al., 1995; Rouchy et al., 2001; Krijgsman et al., 2002; Manzi et al., 2015). In the western Polemi and Pissouri Basins, Tortonian marl successions reflect the progressive shallowing from ~ 500 m at Tortonian/Messinian boundary to < 100 m water depth and marine isolation leading up to the onset of evaporite deposition during the MSC (Kouwenhoven et al., 2006). The gypsum deposits are divided into a lower and upper unit by an intervening breccia horizon (Robertson et al., 1995). The lower unit is predominantly composed of finely-laminated gypsum with evidence for turbidity currents, slumping and debris flows, indicative of sediment reworking down a slope into deeper water. The mega-rudite breccia is formed of metre-scale blocks of fine-grained gypsum in a gypsiferous mark matrix, which Robertson et al. (1995) interpret as large-scale tectonically induced slumping but Rouchy et al. (2001) interpret as the result of karstic dissolution. The overlying upper unit is composed of selenitic gypsum and marl, interpreted as having formed in relatively shallow water. The deposition of these

Upper Gypsums is followed by typical Lago Mare facies sediments, which include palaeosols indicating subaerial exposure during this period (Rouchy et al., 2001). The overlying Zanclean transgressive sediments were deposited in a well-oxygenated deep marine setting (Robertson et al., 1995). Therefore, the Polemi and Pissouri Basins have been traditionally considered to have PLG and Upper Gypsum deposits, based upon the stratigraphic facies constraints. Krijgsman et al. (2002) dated the onset of evaporite formation in the Pissouri Basin at 5.96 Ma using magnetostratigraphy, apparently confirming the synchronous onset of evaporite formation across the Mediterranean. However, recent work by Manzi et al. (2015) concludes that the lower and intermediate units are both the RLG, due to the overall clastic and reworked nature of the facies and that the base of the evaporites dated by Krijgsman et al. (2002) is in fact the MES. In the Maroni sub-basin, the evaporites consist of two distinct units (Robertson et al., 1995) but there is no evidence for late Messinian sediments and the mega-rudite is directly overlain by Pliocene marine marls (Robertson et al., 1995). Therefore, the overall stratigraphy from these basins is very similar to the Hatay Graben, although the Hatay Graben lacks the Upper Gypsum deposits possibly as a result of its more landward position.

Interestingly, directly to the north of the Hatay Graben in the Iskenderun Basin, onshore exposures of gypsum described by Tekin et al. (2010) lack this 'mega-rudite' conglomeratic unit. Instead, the gypsum facies that overly upper Tortonian marls are dominated by laminated gypsums, gypsiferous marls and sandstones, which Tekin et al. (2010) interpret as typical of very shallow water accumulation in lagoons and sabkhas. There are minor selenite accumulations thought to represent slighter deeper water conditions, but overall the Iskenderun basin appears to have had shallower water depths during the MSC than the Hatay Graben. This area could represent the source area for the RLG of the Vakifli Fm., as younger tectonics have dissected the region since deposition (Boulton et al., 2006). Overlying Pliocene deposits are not well described but a thin Lago Mare succession appears to transition upwards into fluvial and coastal environments (Tekin et al., 2010).

Similarly, the Messinian succession in the Adana Basin indicates shallow water or continental conditions. Darbaş and Nazik (2010) and Faranda et al. (2013) describe planktic foraminifera and ostracods from late Miocene sections in the Adana Basin demonstrating that in the early Messinian the area was characterised by shallow coastal environments such as marshes, lagoons and estuaries. Cosentino et al. (2010) recognised a succession of rhythmically bedded anhydrites and black shales that they correlate to the PLG, whereas the outcropping gypsum deposits consist of gypsarenite and gypsrudite containing large blocks of selenite pertaining to the RLG (Radeff et al., 2015). Interestingly, Consentino et al. (2010) also recognise two Messinian erosion surfaces in the Adana Basin; one correlating to the wider MES cutting the lower evaporites, and the other at the base of the overlying continental sequence.

Burton-Ferguson et al. (2005) thought that these continental sediments were Pliocene in age; however, Ilgar et al. (2012) have identified Gilbert-type deltas that are laterally equivalent to the gypsum deposits, and microfossil analysis by Cipollari et al. (2013) and Faranda et al. (2013) showed that these sediments were deposited in brackish water environments of the latest Messinian Lago Mare event. Cipollari et al. (2013) also showed that subsequent Zanclean reflooding resulted in the deposition of deep marine marls in water depths of 200 – 500 m.

6.3 Late Tortonian to Zanclean Palaeoenvironments of the Hatay Graben

It is now possible to synthesise field observations, palaeontological and strontium data with regional trends to develop a model for the late Miocene of the Hatay Graben, which can then be used to test models for the wider Mediterranean at this time.

6.3.1 Late Tortonian to early Messinian

The late Tortonian and earliest Messinian in the Hatay Graben are represented by the Nurzeytin Formation, composed mainly of marl with interbeds of sandstones, from locations 3 and 4 (Figs. 3, 11). These sediments are interpreted as basinal deposition from suspension settling with reworking of material

downslope through the action of slumps, turbidity currents and rare debris flows (Boulton and Robertson, 2007). Boulton et al. (2006) suggested maximum water depths of up to 700 m for this unit; however, our new foraminiferal analysis indicates that by the early Messinian water depths had shallowed to < 200 m in some places and the seabed may have been carpeted in seagrass. This shallowing is potentially due to regional tectonic uplift, sea level fall or to the initiation of local faulting (Boulton et al., 2006), but similar trends have also been recorded in Cypriot basins (Kouwenhoven et al., 2006) resulting from the increasing isolation of the basin. The pre-MSC section on the main road (section 4) is of limited extent so that any changes to planktic foraminifera assemblages prior to the onset of the MSC might not have been identified in this study. Furthermore, it is possible that these pre-MSC sediments have been truncated by an unconformity and younger sediments have been eroded, as indicated by the angular unconformity observed at section 4. The section investigated at Mizrakli (section 3) appears continuous through the Tortonian – Messinian boundary, suggesting that this area may have been protected from later erosion potentially due to a location more proximal to the basin depocentre (Fig. 11).

6.3.2 Stage 1 of the MSC

No gypsum from this period appears to have been preserved *in situ* in the Hatay Graben. Shallow water and sub-aerial gypsum facies have been described north of the Hatay Graben near Iskendurun (Tekin et al., 2010) that are typical of the PLG deposits. PLG and associated deposits have also been described from the Adana Basin, suggesting that PLG could have been deposited if there were suitable conditions at that time. Therefore, it is possible that shallow water deposits were present on the edges of the basin feeding the resedimented gypsum that is observed in the Hatay Graben at the present day, but these deposits have subsequently been eroded. The Plio-Quaternary faulting that has formed the present topographic graben (Boulton and Robertson, 2007) has also dissected the region and previously the Hatay basin may have been part of a wider depositional system that at present.

6.3.3 Stage 2 of the MSC

During Stage 2 of the MSC, it is hypothesised that widespread subaerial erosion took place forming the MES and rivers cut canyons as the fluvial systems adjusted to base level (CIESM, 2008). In the Hatay Graben subaerial exposure led to the erosion of underlying strata (as observed at location 1) in marginal locations at the edge of the basin. Despite this, subsequent deposition of Pliocene sediments and tectonic tilting of the basin makes an evaluation of the lateral extent of the MES difficult due to a lack of exposure (Fig. 11).

In the basin depocentre, formed as a result of active faulting along the southern basin margin, gravity reworking of previously crystallised gypsum led to the formation of the resedimented lower gypsums (RLG). In the Hatay, these deposits consist of two distinct facies associations indicating that a change in the nature of the gravity reworking took place later in this period, resulting in the deposition of the 'mega-clasts' at the end of the RLG period (as indicated by Sr ratios; Tekin et al., 2010). Similar facies are recorded in many locations around the Mediterranean (Sicily, Cyprus, Turkey), which have commonly been attributed to tectonic forcing (i.e., Robertson et al., 1995; Tekin et al., 2010). However, the RLG facies in the Adana Basin have been dated to the early post-evaporitic stage of the MSC (5.55 – 5.45 Ma) owing to the presence of brackish Paratethyan ostracods (Faranda et al., 2013) in the fine-grained interbedded sediments suggesting that downslope transport of clastic gypsum material may have taken place at different times in different basins.

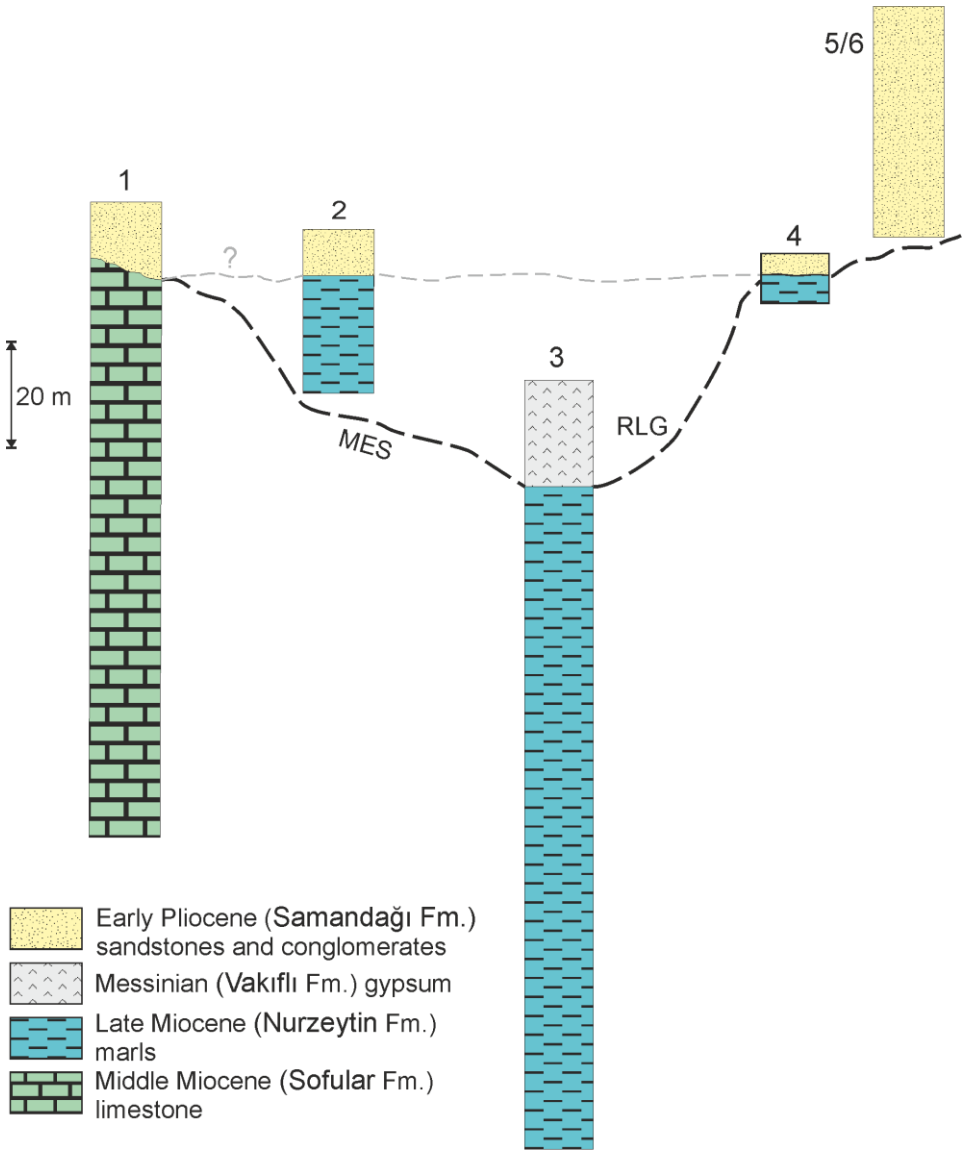

Figure 11. Sketch stratigraphic correlation (horizontal spacing is not to scale) approximately west to east between the key sections (indicated by numbers) discussed in the text and locations shown on figure 3. Note the similarity of the facies described here to the idealised model of the Messinian deposits for a peripheral basin shown in figure 1a. MES – Messinian Erosion Surface, RLG – Resedimented Lower Gypsum.

6.3.4 Stage 3 of the MSC

Although Stage 3 gypsums have been recognised from other eastern Mediterranean basins, the available data suggest that these are lacking in the Hatay Graben owing to either, or probably a combination of: a) later erosion; b) subaerial exposure resulting in a hiatus, or c) water chemistry or other local conditions being unconducive to gypsum formation at this time.

Furthermore, several of the sections studied here have stratigraphic constraints indicating that during the latest Miocene (sections 2, 5, 6) marine conditions may have been present within the Hatay Graben, prior to the Zanclean reflooding. This is in clear contrast to nearby basins on Cyprus and elsewhere in Turkey where UG and/or Lago Mare biofacies deposits have been identified (i.e., Rouchy et al., 2001; Faranda et al., 2013; Manzi et al., 2015; Radeff et al., 2015). Yet Popescu et al. (2009, 2015) and Carnevale et al. (2006) have recorded fossil evidence indicating marine conditions during this period from deep and peripheral basins in the western Mediterranean, supporting the idea that marine conditions returned to the Mediterranean prior to the Pliocene (e.g., Butler et al., 1995; Riding et al., 1998; Bache et al., 2012).

Although further stratigraphic and palaeoenvironmental constraints would be desirable, our available data tentatively support a pre-Pliocene return to marine conditions even in the easternmost Mediterranean.

6.3.5 Zanclean

The base of the Zanclean is normally recognised as the return to marine conditions across the Mediterranean, although as stated above this may not be strictly correct. Available stratigraphic constraints indicate that the earliest Zanclean deposits are composed of interbedded marls and sandstones characteristic of marine conditions and probably represent the deepest water facies in the basin depocentre. Elsewhere, a slightly irregular to planar surface truncates the earlier Miocene marls, forming the base of the sandstone-dominated Samandağ Formation. Coarse-grained sandstones exhibiting a range of facies typical of Gilbert-type deltas or coastal environments generally outcrop stratigraphically above presumably deposited later in the Zanclean (Fig. 11). This dramatic change in facies suggests that although subaerial conditions returned initially in the late Miocene/Pliocene, water depth had shallowed considerably in most of the basin compared to before the MSC. The presence of Gilbert-type fan deltas is indicative of narrow and steep-gradient shelves, possibly infilling the incision developed during stage 2 of the MSC.

7. Conclusions

The available data indicate that the pre-MSC succession of the Hatay Graben is very similar to sequences on Cyprus, and to some extent in Syria, where water depths were likely ≥ 100 m at the onset of the MSC. PLG facies are generally poorly exposed in the eastern Mediterranea and the Hatay Graben is no exception and the gypsum deposits in the Hatay Graben are interpreted as RLG deposits. These lower RLG are often observed to be overlain by a chaotic unit composed of large gypsum 'mega-clasts' observed throughout the eastern Mediterranean and overlying the MES. Robertson et al. (1995), Boulton et al. (2006), and Hardenberg and Robertson (2007) have all previously interpreted these deposits as debris flows potentially triggered by tectonic activity. Although similar central Mediterranean deposits have been classically thought of as having been caused by dissolution collapse, Manzi et al. (2011) has also recently reinterpreted the central Mediterranean breccias as syn-tectonic deposits. This apparent synchronicity raises the question as to how these basins all experienced sediment instability at the same time. If this is the case then the Mediterranean apparently underwent widespread and intense tectonic activity ~ 5.5 Ma. Interestingly, this correlates with proposals that the Arabia-Eurasia collision underwent a period of reorganisation ~ 5 Ma (Allen et al., 2004). However, the Adana Basin also contains evidence for a younger Messinian unconformity, and the RLG deposits in this basin are younger (dating to the Lago Mare biofacies event) than those described elsewhere (Radeff et al., 2015), suggesting that the mega-breccias might span a longer timespan than hitherto recognised. These stratigraphic differences observed north of the Hatay may reflect the proximity of the Adana and Iskenderun basins to the collisional zone between the Arabian and Anatolian micro-plates (the Bitlis-Zagros Suture). Although continental collision was well advanced by the Messinian (e.g., Robertson et al., 2015), the Adana and Iskenderun basins north of the suture zone, would have experienced different uplift and subsidence trajectories than areas to the south (i.e., Hatay and Syria) and the west of the collisional front.

Following deposition of the RLG, the Hatay Graben apparently records evidence for marine conditions at this time in contrast to the other regional basins where Lago Mare facies have been recorded. Although we cannot rule out the presence of typical Lago Mare facies elsewhere in the basin, the apparent presence of marine fauna supports the work of Popescu et al. (2009, 2015) and Carnevale et al. (2006) and others who have proposed a return to marine conditions prior to the Zanclean, though this interpretation needs further corroboration. Finally, regional and local tectonic uplift (e.g., Boulton and Robertson, 2008; Boulton and Whittaker, 2009) meant that the Hatay Graben rapidly shallowed during the Pliocene resulting

in continental or coastal sediments and the deposition of Gilbert-type deltas and associated coastal and fluvial systems.

Therefore, this examination of the Miocene to Pliocene transition outcropping in the Hatay Graben shows that the proposed stratigraphic framework for the whole Mediterranean region is broadly consistent in this easternmost basin. However, questions still remain regarding the timing of the return to marine conditions and the possibility that the refilling of the Mediterranean had commenced by the Zanclean, as well as to the significance of the 'mega-breccias' seen in many regions and their possible connection to the Lago Mare event.

Acknowledgements

SJB acknowledges financial support from the Royal Society and the British Society for Geomorphology for funding field trips where samples were collected. We also thank Alastair Robertson for the introduction to Turkish and Cypriot geology. We thank Prof. U. Ünlügenç for logistical and scientific assistance with this work. We thank the editor and anonymous reviewers for their comments that have improved this manuscript.

References

Allen, M., Jackson, J., Walker, R., 2004. Late Cenozoic reorganization of the Arabia-Eurasia collision and the comparison of short-term and long-term deformation rates. Tectonics 23, DOI: 10.1029/2003TC001530.

Bache, F., Popescu, S.M., Rabineau, M., Gorini, C., Suc, J.P., Clauzon, G., Çakır, Z., 2012. A two-step process for the reflooding of the Mediterranean after the Messinian Salinity Crisis. Basin Research 24, 125-153.

Backert, N., Ford, M., Malartre, F., 2010. Architecture and sedimentology of the Kerinitis Gilbert-type fan delta, Corinth Rift, Greece. Sedimentology 57, 543-586.

Barbieri, R., Ori, G.G., 2000. Neogene palaeoenvironmental evolution in the Atlantic side of the Rifian Corridor (Morocco). Palaeogeography, Palaeoclimatology, Palaeoecology 163, 1-31.

Bassetti, M.A., Manzi, V., Lugli, S., Roveri, M., Longinelli, A., Lucchi, F.R., Barbieri, M., 2004. Paleoenvironmental significance of Messinian post-evaporitic lacustrine carbonates in the northern Apennines, Italy. Sedimentary Geology 172, 1-18.

Blanc P.-L., 2002. The opening of the Plio-Quaternary Gibraltar Strait: Assessing the size of a cataclysm. Geodinamica Acta 15, 303– 317.

Blanc-Valleron, M.M., Rouchy, J.M., Pierre, C., Badaut-Trauth, D., Schuler, M. 1998. Evidence of Messinian Nonmarine deposition at site 968 (Cyprus lower slope). In Robertson, A.H.F., Emeis, K.-C., Richter, C., and Camerlenghi, A. (Eds.), Proceedings of the Ocean Drilling Program Scientific Results Volume 160, 437-446. Available from: http://www.odp.tamu.edu/publications/160_SR/VOLUME/CHAPTERS/CHAP_34.PDF

Blanc-Valleron, M.M., Pierre, C., Caulet, J.P., Caruso, A., Rouchy, J.M., Cespuglio, G., Sprovieri, R., Pestrea S., Di Stefano, E., 2002. Sedimentary, stable isotope and micropaleontological records of paleoceanographic change in the Messinian Tripoli Formation (Sicily, Italy). Palaeogeography, Palaeoclimatology, Palaeoecology 185, 255-286.

Boulton, S.J., 2006. Tectonic-sedimentary evolution of the Cenozoic Hatay Graben, South Central Turkey. University of Edinburgh, unpublished PhD thesis, 414pp.

Boulton, S.J., Robertson, A.H.F., 2007. The Miocene of the Hatay area, S Turkey: Transition from the Arabian passive margin to an underfilled foreland basin related to closure of the Southern Neotethys Ocean. Sedimentary Geology 198, 93-124.

Boulton, S. J., Robertson, A.H.F., 2008. The Neogene-Recent Hatay Graben, South Central Turkey: Oblique-extensional (transtension) graben formation. Geological Magazine 145, 800-821

Boulton S,J. Whittaker, A.C., 2009. Quantifying active faulting in an oblique-extensional graben using geomorphology, drainage patterns and river profiles: Hatay Graben, south central Turkey. Geomorphology 104, 299-316.

Boulton, S.J., Robertson, A.H.F., Unlügenç, Ü.C., 2006. Tectonic and sedimentary evolution of the Cenozoic Hatay Graben, Southern Turkey: A two-phase, foreland basin then transtensional basin model. In: Robertson. A.H.F., Mountrakis, D. (Eds.), Tectonic Evolution of the Eastern Mediterranean. Geological Societyof London, Special Publications 260, pp.613-634.

Boulton, S J., Robertson, A.H.F., Ellam, R.M., Şafak, Ü., Ünlügenç., U.C., 2007. Strontium isotopes and micropalaeontological dating used to redefine the stratigraphy of the Neotectonic Hatay Graben, southern Turkey. Turkish Journal of Earth Sciences 16, 141-180.

Brasier, M.D., 1980. Microfossils. George Allen & Unwin, London, 193pp

Burton-Ferguson, R., Aksu, A.E., Calon, T.J., Hall, J., 2005. Seismic stratigraphy and structural evolution of the Adana Basin, eastern Mediterranean. Marine Geology 221, 189-222.

Butler, R.W.H., Lickorish, W.H., Grasso, M., Pedley, H.M., Ramberti, L., 1995. Tectonics and sequence stratigraphy in Messinian basins, Sicily: Constraints on the initiation and termination of the Mediterranean salinity crisis. GSA Bulletin 107, 425-439.

Carnevale, G., Landini, W., Sarti, G., 2006. Mare versus Lago Mare: marine fishes and the Mediterranean environment at the end of the Messinian Salinity Crisis. Journal of the Geological Society of London 163, 75-80.

CIESM 2008. The Messinian Salinity Crisis from mega-deposits to microbiology - A consensus report. N° 33 in CIESM Workshop Monographs [F. Briand, Ed.], 168 p., CIESM Publisher, Monaco. .

Cimerman, F., Langer, M.R., 1991. Mediterranean foraminifera. S.A.Z.i. Umetnosti. Academia Sciertiarum et Artium Slovenca (Ljubljana) Classis IV, 118 pp.

Cipollari, P., Cosentino, D., Radeff, G., Schildgen, T.F., Faranda, C., Grossi, F., Gliozzi, E., Echtler, H., 2013. Easternmost Mediterranean evidence of the Zanclean flooding event and subsequent surface uplift: Adana Basin, southern Turkey. In: Robertson, A.H.F., Parlak, O., Ünlügenç., U.C (eds). Geological Development of Anatolian an the Easternmost Mediterranean Region. Geological Society, London, Special Publications 372, pp. 473-494.

Clauzon, G., Suc, J.P., Gautier, F., Berger, A., Loutre, M. F., 1996. Alternate interpretation of the Messinian salinity crisis: Controversy resolved?. Geology, 24(4), 363-366.

Clifton, H. E., 2006. A re-examination of facies models for clastic shorefaces. In: Posamentier, H.W., Walker, R.G. (Eds.), Facies Models Revisited, Special Publication No. 84, SEPM (Society for Sedimentary Geology), Tulsa, USA. pp. 293–337

Cosentino, D., Darbas, G., Gürbüz, K., 2010. The Messinian salinity crisis in the marginal basins of the peri-Mediterranean orogenic systems: examples from the central Apennines (Italy) and the Adana Basin (Turkey). Geophysical Research Abstracts 12, EGU2010-2462.

Darbaş, G., Nazik, A., 2010. Micropaleontology and paleoecology of the Neogene sediments in the Adana Basin (South of Turkey). Journal of Asian Earth Sciences 39, 136-147.

Dashtgard, S.E. MacEachern, J.A., Frey, S.E., Gingras, M.K., 2012. Tidal effects on the shoreface: Towards a conceptual framework. Sedimentary Geology 279, 42–61.

De Lange, G.J., Krijgsman, W., 2010. Messinian salinity crisis: a novel unifying shallow gypsum/deep dolomite formation mechanism. Marine Geology 275, 273–277.

Dela Pierre, F., Bernardi, E., Cavagna, S., Clari, P., Gennari, R., Irace, A., Lazar, F., Lugli, S., Manzi, V., Natalicchio, M., Roveri, M.,Violanti, D., 2011. The record of the Messinian salinity crisis in the Tertiary Piedmont Basin (NW Italy): The Alba section revisited. Palaeogeography, Palaeoclimatology, Palaeoecology 310, 238-255.

Dela Pierre, F., Clari, P., Bernardi, E., Natalicchio, M., Costa, E., Cavagna, S., Lozar, F., Lugli, S., Manzi, V., Roveri, M., Violanti, D., 2012. Messinian carbonate-rich beds of the Tertiary Piedmont Basin (NW Italy): microbially-mediated products straddling the onset of the salinity crisis. Palaeogeography, Palaeoclimatology, Palaeoecology 344, 78-93.

Duggen, S., Hoernle, K., Van Den Bogaard, P., Rüpke, L., Morgan, J.P., 2003. Deep roots of the Messinian salinity crisis. Nature 422, 602-606.

Eaton, S., 1987. The sedimentology of mid to late Miocene carbonates and evaporites in Southern Cyprus. PhD dissertation, University of Edinburgh, 323 pp.

Estrada, F., Gorini, C., Ercilla, G., Ammar, A., Alonso, B., Maldonado, A., Vázquez, J.T., 2011. New insights into the Messinian salinity crisis: Zanclean reflooding erosion in the Gibraltar-Alboran Sea connection area. 13th Congress RCMNS (International Union of Geological Sciences), Earth System Evolution and the Mediterranean area from 23Ma to present. Naples, (Italy), 2-6 September 2009.

Faranda, C., Gliozzi, E., Cipollari, P., Grossi, F., Darbaş, G., Gürbüz, K., Nazik, A. Gennari, R., Cosentino, D., 2013. Messinian paleoenvironmental changes in the easternmost Mediterranean: a case study in the Adana Basin (southern Turkey). Turkish Journal of Earth Sciences 22, 839-863.

Fisher, R.A., Corbet, A.S., Williams, C.B. 1943. The relation between the number of species and the number of individuals in a random sample of an animal population. The Journal of Animal Ecology 12, 42-58.

Flecker, R., Ellam, R.M., 2006. Identifying Late Miocene episodes of connection and isolation in the Mediterranean–Paratethyan realm using Sr isotopes. Sedimentary Geology 188–189, 189–203.

Flecker, R., Ellam, R.M., Müller, C., Poisson, A., Robertson, A.H.F., Turner, J., 1998). Application of Sr isotope stratigraphy and sedimentary analysis to the origin and evolution of the Neogene basins in the Isparta Angle, southern Turkey. Tectonophysics 298, 83-101.

Follows, E.J., 1992. Patterns of reef sedimentation and diagenesis in the Miocene of Cyprus. Sedimentary Geology 79, 225-253.

Garcia-Castellanos, D., Estrada, F., Jiménez-Munt, I., Gorini, C., Fernàndez, M., Vergés, J., de Vicente, R. 2009. Catastrophic flood of the Mediterranean after the Messinian salinity crisis. Nature 462, 778–781.

Gennari, R., Iaccarino, S.M., Di Stefano, A., Sturiale, G., Cipollari, P., Manzi, V., Roveri , M., Cosentino, D., 2008. The Messinian–Zanclean boundary in the Northern Apennines. Stratigraphy 5, 307-322.

Govers, R., Meijer, P., Krijgsman, W., 2009. Regional isostatic response to Messinian Salinity Crisis events. Tectonophysics 463, 109-129

Grossi, F., Cosentino, D., Gliozzi, E., 2008. Late Messinian Lago Mare ostracods and palaeoenvironments of the central and eastern Mediterranean Basin. Bulletin Societie de Paleontologia Italia 47, 131-146

Hardenberg, M.F., Robertson, A.H., 2007. Sedimentology of the NW margin of the Arabian plate and the SW–NE trending Nahr El-Kabir half-graben in northern Syria during the latest Cretaceous and Cenozoic. Sedimentary Geology 201, 231-266.

Hardenberg, M.F., Robertson, A.H., 2013. Role of the Palaeogene–Recent sinistral El-Kabir Lineament and the associated transtensional Neogene–Recent El-Kabir Basin (northern Syria) in distributed deformation between the African and Eurasian plates. Geological Society, London, Special Publications, 372(1), 447-471.

Hilgen, F.J., Krijgsman, W., 1999. Cyclostratigraphy and astrochronology of the Tripoli diatomite formation (pre-evaporite Messinian, Sicily, Italy). Terra Nova 11, 16-22.

Hilgen, F.J., Bissoli, L., Iaccarino, S., Krijgsman, W., Meijer, R., Negri, A., Villa, G., 2000. Integrated stratigraphy and astrochronology of the Messinian GSSP at Oued Akrech (Atlantic Morocco). Earth and Planetary Science Letters 182, 237-251.

Hilgen, F.J., Kuiper, K., Krijgsman, W., Snel, E., van der Laan, E., 2007. Astronomical tuning as the basis for high resolution chronostratigraphy: the intricate history of the Messinian salinity crisis. Stratigraphy 4, 231–238.

Hsü, K.J., 1973. The desiccated deep-basin model for the Messinian events. In: Drooger, C.W. (ed.) Messinian events in the Mediterranean, North-Holland Pub. Co, Amsterdam. 60-67 pp.

Iaccarino, S., Castradoti, D., Cita, M.B., Di Stafano, E., Gaboardi, S., McKenzie, J.A., Spezzaferri, S., Sprovieri, R., 1999a. The Miocene-Pliocene boundary and the significance of the earliest Pliocene flooding in the Mediterranean. Memoire della Società Geologica Italiana 54, 109-131.

Iaccarino, S., Cita, M.B., Gaboardi, S., Gruppini, G.M., 1999b. High-resolution biostratigraphy at the Miocene/Pliocene boundary in holes 974B and 975B, Western Mediterranean. In: Zahn, R., Comas, M.C., Klaus, A. (Eds.), Proceedings of the Ocean Drilling Program, Scientific Results 161, pp. 197-221.

Ilgar, A., Nemec, W., Hakyemez, A., Karakuş, E., 2013. Messinian forced regressions in the Adana Basin: a near-coincidence of tectonic and eustatic forcing. Turkish Journal of Earth Science 22, 864-889.

Kouwenhoven, T.J., Morigi, C., Negri, A., Giunta, S., Krijgsman, W., Rouchy, J.M. 2006. Paleoenvironmental evolution of the eastern Mediterranean during the Messinian: constraints from integrated microfossil data of the Pissouri Basin (Cyprus). Marine Micropaleontology 60, 17-44.

Krijgsman, W., Hilgen, F.J., Raffi, I., Sierro, F.J., Wilson, D.S., 1999. Chronology, causes and progression of the Mediterranean salinity crisis. Nature 400, 652–655.

Krijgsman, W., Blanc-Valleron, M.M., Flecker, R., Hilgen, F.J., Kouwenhoven, T.J., Merle, D., Orszag-Sperber, F., Rouchy, J.M., 2002. The onset of the Messinian salinity crisis in the Eastern Mediterranean (Pissouri Basin, Cyprus). Earth and Planetary Science Letters 194, 299-310.

Lazar, M., Schattner, U., Reshef, M., 2012. The great escape: An intra-Messinian gas system in the eastern Mediterranean. Geophysical Research Letters 39, L20309, doi:10.1029/2012GL053484

Loget, N., Van Den Driessche, J., 2006. On the origin of the Strait of Gibraltar. Sedimentary Geology 188, 341– 356.

Lourens, L.J., Hilgen, F.J., Laskar, J., Shackleton, N. J., Wilson, D., 2004. The Neogene period. In: Gradstein, F., Ogg, J., et al. (Eds.), A Geologic Time Scale. Cambridge University Press, UK. pp.409-440.

Lugli, S., Manzi, V., Roveri, M., 2008. New facies interpretation of the Messinian evaporites in the Mediterranean. In: CIESM 2008. The Messinian Salinity Crisis from mega-deposits to microbiology - A consensus report. N° 33 in CIESM Workshop Monographs [F. Briand, Ed.], CIESM Publisher, Monaco pp. 67-72).

Lugli, S., Manzi, V., Roveri, M., Schreiber, B.C., 2010. The Primary Lower Gypsum in the Mediterranean: a new facies interpretation for the first stage of the Messinian salinity crisis. Palaeogeography, Palaeoclimatology, Palaeoecology 297, 83–99.

Lutze, G.F., Coulbourn, W.T., 1984. Recent benthic foraminifera from the continental margin of northwest Africa: community structure and distribution. Marine Micropaleontology 8, 361-401.

Manzi, V., Roveri, M., Bertini, A., Biffi, U., Giunta, S., Iaccarino, S.M., Lanci, L., Lugli, S., Negri, A., Riva, A., Rossi, M.E., Taviani, M., 2007. The deep-water counterpart of the Messinian Lower Evaporites in the Apennine foredeep: the Fanantello section (Northern Apennines, Italy). Palaeogeography, Palaeoclimatology, Palaeoecology 251, 470–499.

Manzi, V., Lugli, S., Roveri, M., Charlotte Schreiber, B., 2009. A new facies model for the Upper Gypsum of Sicily (Italy): chronological and palaeoenvironmental constraints for the Messinian salinity crisis in the Mediterranean. Sedimentology 56, 1937-1960.

Manzi, V., Lugli, S., Roveri, M., Schreiber, B.C., Gennari, R., 2011. The Messinian "Calcare di Base" (Sicily, Italy) revisited. Geological Society of America Bulletin 123, 347-370.

Manzi, V., Gennari, R., Hilgen, F., Krijgsman, W., Lugli, S., Roveri, M., Sierro, F.J., 2013. Age refinement of the Messinian salinity crisis onset in the Mediterranean. Terra Nova 25, 315-322.

Manzi, V., Lugli, S., Roveri, M., Dela Pierre, F., Gennari, R., Lozar, F., Natalicchio, M., Schreiber, B.C., Taviani, M. Turco, E., 2015. The Messinian salinity crisis in Cyprus: a further step toward a new stratigraphic framework for Eastern Mediterranean. Basin Research DOI: 10.1111/bre.12107.

Meijer P.T., Krijgsman W., 2005. A quantitative analysis of the desiccation and refilling of the Mediterranean during the Messinian Salinity Crisis. Earth and Planetary Science Letters 240, 510–520.

Melinte-Dobrinescu, M.C., Suc, J.P., Clauzon, G., Popescu, S.M., Armijo, R., Meyer, B., Çakir, Z. 2009. The Messinian salinity crisis in the Dardanelles region: Chronostratigraphic constraints. Palaeogeography, Palaeoclimatology, Palaeoecology 278, 24-39.

Milker, Y., & Schmiedl, G., 2012. A taxonomic guide to modern benthic shelf foraminifera of the western Mediterranean Sea. Palaeontologia Electronica 15, 1-134.

Murray, J.W., 1976. A method of determining proximity of marginal seas to an ocean. Marine Geology 22, 103-119.

Murray, J.W., 1991. Ecology and Palaeoecology of Benthic Foraminifera. Longman, Harlow, Essex, 397pp.

Murray, J.W., 2006. Ecology and applications of benthic foraminifera, Cambridge University Press, New York, Cambridge, 426pp.

Orszag-Sperber, F., 2006. Changing perspectives in the concept of "Lago Mare" in Mediterranean Late Miocene evolution. Sedimentary Geology 188–189, 259–277.

Payne, A.S., Robertson, A.H.F., 1995. Neogene supra-subduction zone extension in the Polis Graben system, west Cyprus. Journal of the Geological Society of London 152, 613-628.

Periáñez, R., Abril, J.M., 2015. Computational fluid dynamics simulations of the Zanclean catastrophic flood of the Mediterranean (5.33 Ma). Palaeogeography, Palaeoclimatology, Palaeoecology 424, 49-60.

Pierre, C., Caruso, A., Blanc-Valleron, M. –M., Rouchy, J. M., Orszag-Sperber, F., 2006. Reconstruction of the Palaeoenvironmental changes around the Miocene-Pliocene boundary along a West-east transect across the Mediterranean. Sedimentary Geology 188-189, 319-340.

Pierre, C., Rouchy, J. M., Blanc-Valleron, M.–M., 1998. Sedimentological and stable isotope changes at the Messinian/Pliocene boundary in the Eastern Mediterranean (holes 968A, 969A, and 969B). In: Robertson, A. H. F., Emeis, K. –C., Richter, C., Camerlenghi, A., (Eds.), Proceedings of the Ocean Drilling Program 160, pp.3-8.

Poisson, A., Orszag-Sperber, F., Kosun, E., Bassetti, M. A., Müller, C., Wernli, R., Rouchy, J.M., 2011. The Late Cenozoic evolution of the Aksu basin (Isparta Angle; SW Turkey). New insights. Bulletin de la Societe Geologique de France 182, 133-148.

Popescu, S. M., Dalesme, F., Jouannic, G., Escarguel, G., Head, M.J., Melinte-Dobrinescu, M.C., Sütö-Szentai, M., Bakrac, K., Clauzon, G., Suc, J.-P., 2009. *Galeacysta etrusca* complex: dinoflagellate cyst marker of Paratethyan influxes to the Mediterranean Sea before and after the peak of the Messinian Salinity Crisis. Palynology 33, 105-134.

Popescu, S.M., Dalibard, M., Suc, J.P., Barhoun, N., Melinte-Dobrinescu, M.C., Bassetti, M.A., Deaconu, F., Head, M.J., Gorini, C., Do Couto, D., Rubino, J-L., Auxietre, J-L., Floodpage, J., 2015. Lago Mare episodes around the Messinian–Zanclean boundary in the deep southwestern Mediterranean. Marine and Petroleum Geology 15, 55-70.

Sanders, D., 2000. Rocky shore-gravelly beach transition, and storm/post-storm changes of a Holocene gravelly beach (Kos Island, Aegean Sea): stratigraphic significance. Facies 42, 227-244.

Radeff, G., Cosentino, D., Cipollari, P., Schildgen, T.F., Iadanza, A., Srecker, M., Darbas, G., Gürbüz, K., 2015. Stratigraphic architecture of ther upper Messinian deposits of the Adana Basin (Southern Turkey): implications for the Messinian salinity crisis and the Taurus petroleum system. Italian Journal of Geosciences doi:10.3301/IJG.2015.18

Reading, H.G., Collinson, J.D., 1996. Clastic coasts. In: Reading, H.G. (Ed), Sedimentary Environments: Processes, Facies and Stratigraphy, 3rd edition. Blackwell Science, Oxford, pp.154-231.

Riding, R., Braga, J.C., Martín, J.M., Sánchez-Almazo, I.M., 1998. Mediterranean Messinian Salinity Crisis: constraints from a coeval marginal basin, Sorbas, Southeastern Spain. Marine Geology 146, 1-20.

Robertson, A.H.F., Clift, P.D., Degnan, P.J., Jones, G., 1991. Palaeogeographic and palaeotectonic evolution of the Eastern Mediterranean Neotethys. Palaeogeography Palaeoclimatology Palaeoecology 87, 289-343.

Robertson, A.H.F., Eaton, S., Follows, E.J., Payne, A.S., 1995. Depositional processes and basin analysis of Messinian evaporites in Cyprus. Terra Nova 7, 233-253.

Robertson, A.H.F., Boulton, S.J., Taslı, K., Yıldırım, N., İnan, N., Yıldız, A., Parlak, O., 2015. Late Cretaceous-Miocene sedimentary development of the Arabian continental margin in SE Turkey (Adıyaman Region): implications for regional palaeogeography and the closure history of Southern Neotethys. Journal of Asian Earth Sciences. doi:10.1016/j.jseaes.2015.01.025.

Rouchy, J.M., Caruso, A., 2006. The Messinian salinity crisis in the Mediterranean basin: a reassessment of the data and an integrated scenario. Sedimentary Geology 188–189, 35–67.

Rouchy, J.M., Orszag-Sperber, F., Blanc-Valleron, M.–M., Pierre, C., Rivière, M., Combourieu-Nebout, N., Panayides, I., 2001. Palaeoenvironmental changes at the Messinian-Pliocene boundary in the eastern Mediterranean (southern Cyprus basins): significance of the Messinian Lago Mare. Sedimentary Geology 145, 93-117.

Rouchy, J.M., Pierre, C., Et-Touhami, M., Kerzazi, K., Caruso, A., Blanc-Valleron, M-M., 2003. Late Messinian to Early Pliocene palaeoenvironmental changes in the Melilla Basin (NE Morocco) and their relation to Mediterranean evolution. Sedimentary Geology 163, 1-27.

Roveri, M., Lugli, S., Manzi, M., Schreiber, B.C., 2008a. The Messinian Sicilian stratigraphy revisited: new insights for the Messinian salinity crisis. Terra Nova 20 483–488.

Roveri, M., Bertini, A., Cosentino, D., Di Stefano, A., Gennari, R., Gliozzi, E., Grossi, F., Iaccarino, S.M., Lugli, S., Manzi, V., Taviani, M., 2008b. A high-resolution stratigraphic framework for the latest Messinian events in the Mediterranean area. Stratigraphy 5, 323–342.

Roveri, M., Flecker, R., Krijgsman, W., Lofi, J., Lugli, S., Manzi, V., Sierro, F.J., Bertini, A., Camerlenghi, A., De Lange, G., Govers, R., Hilgen, F.J., Hubsher, C., Meijer, P.T., Stoica, M., 2014a. The Messinian Salinity Crisis: Past and future of a great challenge for marine sciences. Marine Geology 352, 25-58.

Roveri, M., Lugli, S., Manzi, V., Gennari, R., Schreiber, B.C. 2014b. High-resolution strontium isotope stratigraphy of the Messinian deep Mediterranean basins: Implications for marginal to central basins correlation. Marine Geology 349, 113-125.

Ruggieri, G., 1967. The Miocene and later evolution of the Mediterranean Sea. In: Adams, C.G. Ager D.V. (Eds.), Aspects of Tethyan Biogeography, Systematic Association special publications 7, pp. 283–290

Sen Gupta, B. K., Machain-Castillo, M. L., 1993. Benthic foraminifera in oxygen-poor habitats Marine Micropaleontology 20, 183-201.

Sierro, F.J., Flores, J.A., Zamarreno, I., Vazquez, A., Utrilla, R., Francés, G., Hilgen, F.J., Krijgsman, W., 1999. Messinian pre-evaporite sapropels and precession-induced oscillations in western Mediterranean climate. Marine Geology 153, 137-146.

Sierro, F.J., Hilgen, F.J., Krijgsman, W., Flores, J.A., 2001. The Abad composite (SE Spain): a Messinian reference section for the Mediterranean and the APTS. Palaeogeography, Palaeoclimatology, Palaeoecology 168, 141–169.

Sierro, F.J., Flores, J.A., Francés, G., Vazquez, A., Utrilla, R., Zamarreño, I., Erlenkeuser, H., Barcena, M. A., 2003. Orbitally-controlled oscillations in planktic communities and cyclic changes in western Mediterranean hydrography during the Messinian. Palaeogeography, Palaeoclimatology, Palaeoecology 190, 289-316.

Sierro, F.J., Ledesma S., Flores J.A., 2008. Astrobiochronology of Late Neogene deposits near the Strait of Gibraltar (SW Spain). Implications for the tectonic control of the Messinian Salinity Crisis. In:

Briand, F. (Ed.) The Messinian Salinity Crisis from mega-deposits to microbiology - A consensus report. N° 33 in CIESM Workshop Monographs, CIESM Publisher, Monaco, pp.45-49.

Stow, D.A.V., Reading, H.G., Collinson, J.D., 1996. Deep Seas. In: Reading, H.G. (Ed), Sedimentary Environments: Processes, Facies and Stratigraphy, 3rd edition. Ed: H.G. Reading. Blackwell Science, Oxford, pp.395-453.

Tekin, E., Varol, B., Ayyıldız, T., 2010. Sedimentology and paleoenvironmental evolution of Messinian evaporites in the Iskenderun–Hatay basin complex, Southern Turkey. Sedimentary Geology 229, 282-298.

Van Couvering, J.A., Castradori, D., Cita, M.B., Hilgen, F.J., Rio D., 2000. The base of the Zanclean Stage and of the Pliocene Series. Episodes 23, 179–187.

Vai, G.B., Ricci Lucchi, F., 1977. Algal crusts, autochthonous and clastic gypsum in a cannibalistic evaporite basin: a case history from the Messinian of Northern Apennines. Sedimentology 24, 211–244

Warren, J.K., 2006. Evaporites: sediments, resources and hydrocarbons. Springer Publications, Berlin. 1035p.

Williams, C.B., 1964. Patterns in the Balance of Nature and Related Problems in Quantitative Ecology. Academic Press, New York.

Zieman, J.C., Zieman, R.T., 1989. The ecology of the seagrass meadows of the west coast of Florida: a community profile (No. BR-85 (7.25)). Fish and Wildlife Service, Washington, D.C. (USA); Virginia Univ., Charlottesville, VA (USA). Dept. of Environmental Sciences. 155pp.